Theses and Dissertations	1. Thesis and Dissertation Collection, all items

1969-06

The effect of wick geometry on the operation of a longitudinal heat pipe.

Kilmartin, Hugh Edward Jr.

Monterey, California. U.S. Naval Postgraduate School

http://hdl.handle.net/10945/12072

THE EFFECT OF WICK GEOMETRY ON THE
OPERATION OF A LONGITUDINAL HEAT PIPE

by

Hugh Edward Kilmartin

United States
Naval Postgraduate School

THESIS

THE EFFECT OF WICK GEOMETRY

ON THE OPERATION OF A

LONGITUDINAL HEAT PIPE

by

Hugh Edward Kilmartin, Jr.

June 1969

This document has been approved for public re-
lease and sale; its distribution is unlimited.

The Effect of Wick Geometry

on the Operation of a

Longitudinal Heat Pipe

by

Hugh Edward Kilmartin, Jr.
Lieutenant (junior grade), United States Navy
B.S., Naval Academy, 1968

Submitted in partial fulfillment of the
requirements for the degree of

MASTER OF SCIENCE IN MECHANICAL ENGINEERING

from the

NAVAL POSTGRADUATE SCHOOL
June 1969

ABSTRACT

Evaporative heat transfer limits were obtained and
studied for an everted heat pipe with varying wick geo-
metries. The wick geometries were a function of the wire
mesh size and the total wick thickness.

A nickel heat pipe was built and operated using both
water and ethyl alcohol as the working fluids. The
different wick materials used were 50 mesh, 80 mesh,
and 150 mesh, plain weave, nickel wire cloth. The scope
of the investigation included operating the pipe at
25 inches mercury vacuum, 10 inches mercury vacuum, and
5 pounds per square inch gage.

The maximum heat transfer was found to increase as
the mesh size was decreased, as the wick thickness was
increased, or as the pressure was increased.

The equipment used to obtain experimental data is
described and experimental results and sample calcula-
tions are presented.

TABLE OF CONTENTS

LIST OF TABLES

LIST OF FIGURES

TABLE OF SYMBOLS

b   - Wick permeability coefficient

L   - Pipe length

$\dot{m}$ - Mass flow rate

N_f - Working fluid parameter

N_m - Inverse of wick permeability

N_{Rr} - Reynolds number

P_L - Liquid pressure

P_V - Vapor pressure

Q   - Heat transfer rate

r_c - Capillary radius

r_g - Inner radius of glass envelope

r_i - Radius of wick-pipe interface

r_o - Outer radius of the wick

r_v - Radius of vapor space in a pipe

R   - Radius of curvature

s   - Numerical coefficient for evaporation and condensation

T   - Temperature

z   - Axial direction of pipe

γ - Surface tension

ε - Wick porosity

θ - Wetting angle

μ - Viscosity

λ - Heat of vaporization

ρ - Density

SUBSCRIPTS

c   - Condenser

e   - Evaporator

eff - Effective

f   - Liquid

max - Maximum

min - Minimum

opt - Optimum

v   - Vapor

ACKNOWLEDGEMENTS

I. INTRODUCTION

In 1942, while working for General Motors, Gaugler investigated the principle of what is now called the heat pipe [5].[*] The first published article did not appear until 1964, however, when Grover studied heat pipes at the Los Alamos Scientific Laboratory [8]. Grover found that heat pipes can transfer thermal energy with a very high efficiency compared to the efficiency of a solid conductor. For example, a temperature drop of only eleven degrees was encountered when a two foot long molybdenum heat pipe transferred forty five hundred watts at a temperature of 2642°F. The energy transferred per unit weight for such a device is over five hundred times that of a solid conductor [7].

A heat pipe consists of a closed container with a liquid-saturated wick that lines its inner walls. The physical properties of the heat pipe vary widely, as the principle of the heat pipe is valid for a variety of containment vessels, fluids, and wicking materials. Containment vessels have been made of materials such as glass, tungsten, and various alloys. Liquid nitrogen and silver have both been used as working fluids. Wicking materials have included woven mesh, fiber glass, and packed beads.

---

[*]Numbers in brackets refer to numbered references in Bibliography.

Operating temperatures as high as 3632°F have been attained
[15], and as low as -319°F [2]. The most common shape of
a heat pipe is cylindrical, but space oriented projects
require the study of heat pipes as low weight radiator
fins.

In operation, a heat pipe transfers thermal energy from
a heat source to a heat sink. A basic diagram of an operating
heat pipe is shown in Figure 1.

PIPE WALL   WICK

HEAT SOURCE   VAPOR SPACE   HEAT SINK
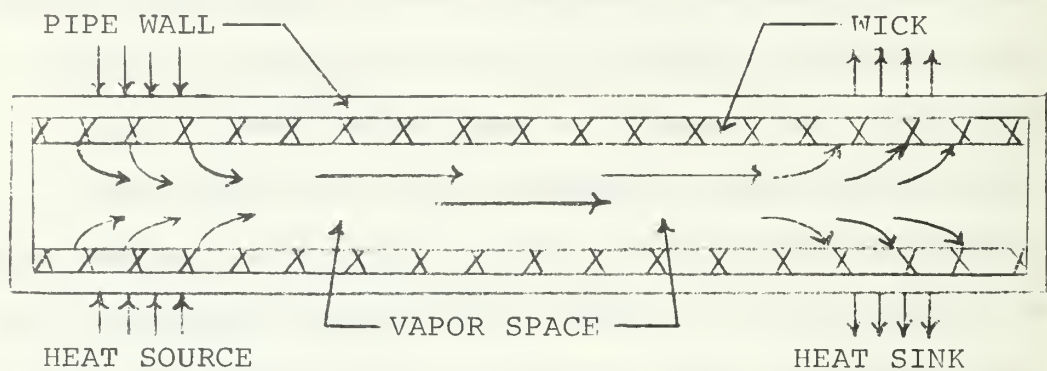
Figure 1. Schematic of Basic Heat Pipe

The temperature difference between the heat source and
liquid-vapor interface is large enough to cause the flow
of thermal energy by radial conduction. At the liquid-
vapor interface the liquid is vaporized, transporting the
thermal energy into the vapor space as latent heat. The
local pressure rises slightly when the vapor is formed,
and a small vapor pressure gradient is created between the
condenser and evaporator sections, which drives the vapor
to the condenser section. As the vapor reaches the liquid-
vapor interface in the condenser it encounters a slightly
lower temperature. The vapor then condenses, losing its

14

latent heat. The pressure in the condenser section drops slightly as the vapor condenses, and the pressure gradient from the evaporator to the condenser end is conserved. At the same time a temperature gradient is produced between the liquid-vapor interface and the heat sink, causing thermal energy to flow from the heat pipe. So far everything described has been applicable to any boiler or steam-heating arrangement. The final step to complete the process is to transport the liquid condensate from the condenser to the evaporator. In conventional systems either a pump is used to force the liquid back to the heat source, or the fluid is allowed to flow back utilizing gravity. The heat pipe, however, is characterized by its unique method of condensate return. The wicking structure, using the surface tension of the fluid and the small pore openings in its own structure, pumps the liquid back to the evaporator by capillary action. This completes the cycle.

There are several obvious advantages to such a system. It can operate with or without the presence of gravity and has no moving parts. This makes it attractive for use in a space environment. Another advantage is that the working fluid has a high heat of vaporization compared to its specific heat, meaning that only a small temperature differ-ence is required to transport a large amount of thermal energy. Also, the temperature of the vaporized fluid remains constant as it flows from the evaporator to the condenser, tending to hold the entire pipe at a constant

15

temperature. It is these last two features which account for the high thermal conductance exhibited by heat pipes.

There are two main causes of breakdown for the system just described. A radial limit is reached when the heat flux from the source is large enough to cause the formation of vapor bubbles in the wick. This will disrupt the return of fluid to the evaporator. The disruption is greatly magnified if the pore openings in the wick are so small that the vapor bubbles are trapped inside the wick. When the return fluid flow is impeded, the evaporator does not receive enough coolant and the temperature there will rise rapidly.

The axial heat flux of the system is limited by entrainment, sonic velocity, and the capillary pumping limit in the wick. Entrainment occurs when the vapor flow picks up liquid from the wick-vapor interface and returns it to the condenser. Pipe operation is limited when entrainment becomes so dominant that an insufficient amount of liquid is returned to the evaporator, causing the temperature there to rise. The vapor flow may also reach the speed of sound, in which case the axial heat flux would again be limited. The limitations of entrainment and sonic velocity are important when the vapor flow in the pipe is significant. For low temperature heat pipes, as used in this study, the vapor pressure drop is insignificant when compared to the liquid pressure drop in the wick. The magnitude of the axial heat flux, then, is limited by the

maximum pumping capabilities of the wick. The evaporator

heat flux can be increased until the maximum capillary

pumping force created by the wick equals the drag caused

by the liquid flowing through the wick. When more heat is

added, the liquid is evaporated faster than the wick can

replace it. Thus, the evaporator dries out and begins

to rise in temperature.

A.   OBJECT

The purpose of this investigation was to study the

effects of the wicking structure properties that are

thought to be important on the maximum axial heat transfer

limitation. Several meshes of plain weave wire cloth in

conjunction with various wick thicknesses were investigated.

II. DESCRIPTION OF EQUIPMENT

With the object of the study in mind, the heat pipe used for this investigation was designed by W. L. Mosteller [16]. It is an everted heat pipe; that is, the heat source and heat sink are on the inside of the pipe, while the wick is wrapped around the outside. The entire pipe, including the vapor space, is enclosed in a glass containing envelope which allows visual observation of the wick. Figure 2 is a sectional view of the everted heat pipe, and Figure 3 is a photograph of the device.

The containing tube is a .750 inch O.D., type "A" nickel, cold drawn, seamless tube with a .065 inch wall thickness. The tube is eighteen inches long with an actual working length of fourteen inches. The fourteen inch length is split into sections of nine inches and five inches by a metal plug welded inside the tube. The five inch section contains the evaporator and adiabatic portion, consisting of a cartridge heater, rated at 500 watts, and a one-half inch thickness of asbestos. The power delivered to the heater was controlled by a variac and measured by an AC wattmeter. The heater was only one-half inch in diameter, so a copper sleeve was inserted between the heater and the inside of the pipe to provide a close fit and an even temperature distribution. The sleeve and heater were both treated with an anti-seize compound

18
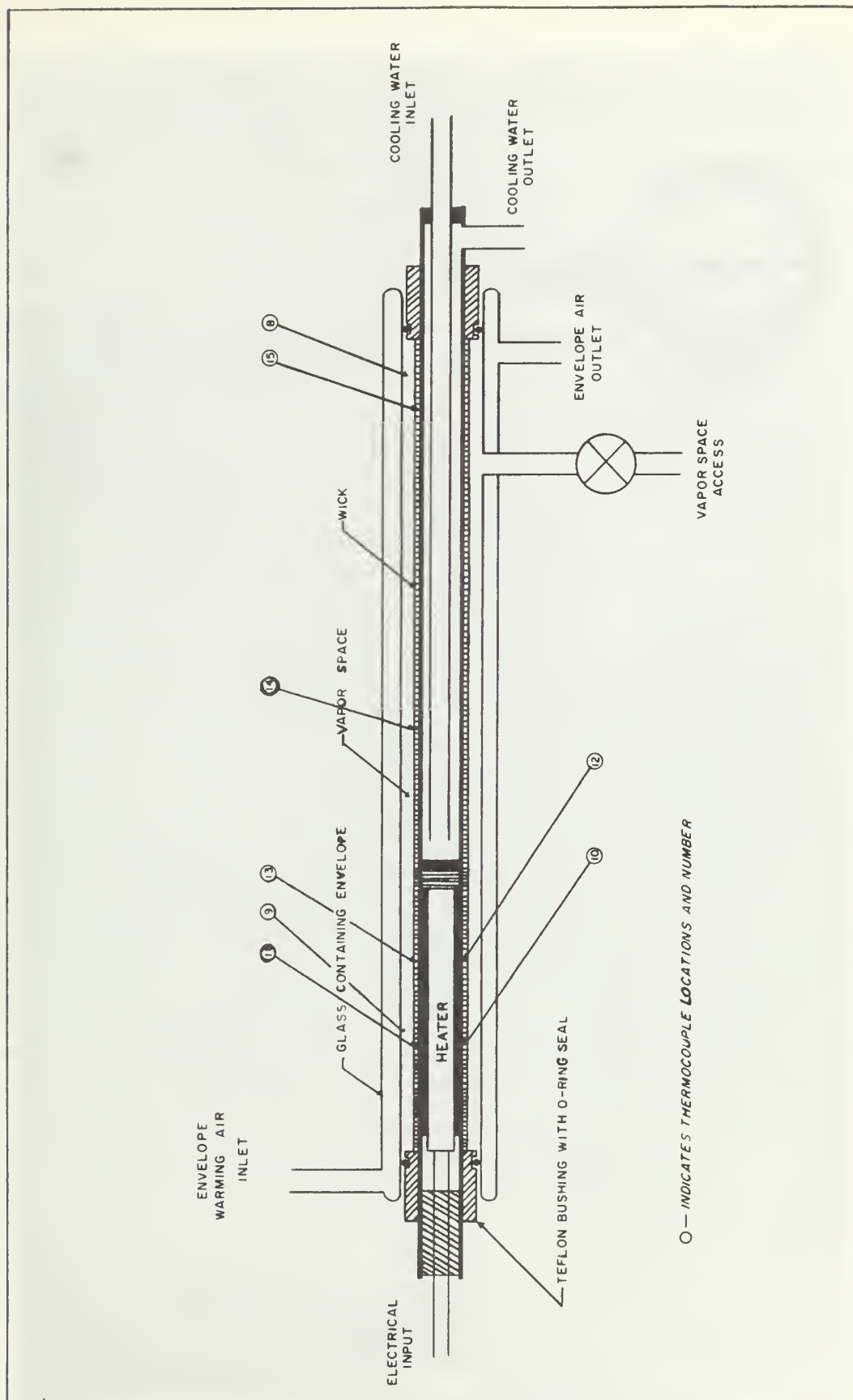
Fig 2 Sectional View of Everted Heat Pipe

19
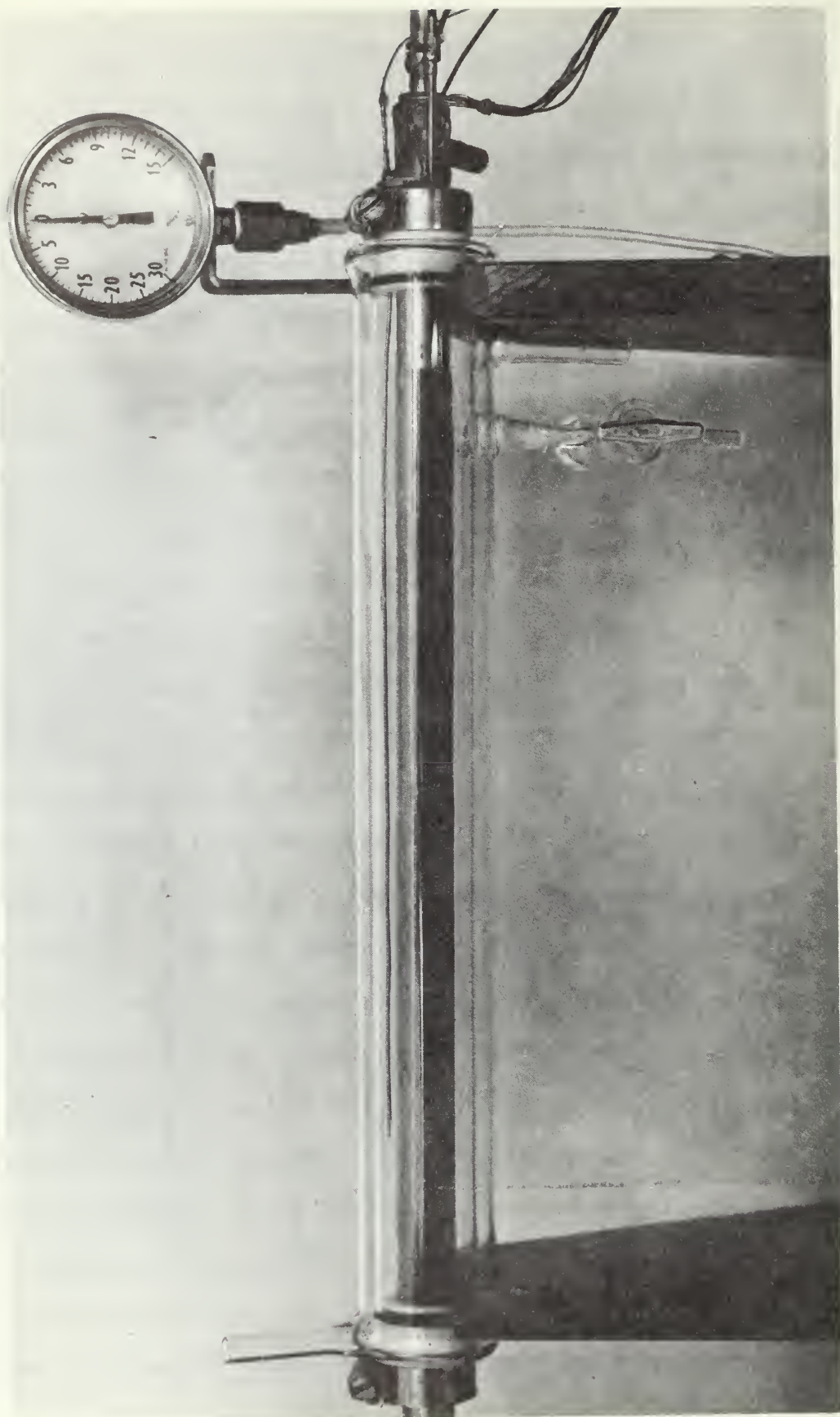
Figure 3. Photograph of Everted Heat Pipe

20

before insertion into the pipe. The nine inch section
served as the condenser of the pipe. Cooling water
entered through the center tube of a return flow annular
design and collected heat from the pipe as it passed back
through the annulus. The flow rate was measured by a flow
rotameter.

A glass evelope, 1.88 inch O.D. and 1.34 inch I.D.,
with an annular space of .16 inches, enclosed the system.
The concentric tubes were sealed at both ends, thereby
sealing the annular space. Temperature controlled air
was pumped through the .16 inch annular section by a
diaphragm-type air compressor. A variac-controlled heater
heated the air in a small chamber until it was a few
degrees above the saturation temperature of the fluid in
the system. The warm air raised the temperature of the
glass envelope and prevented the working fluid from con-
densing on the inner surface of the annulus. The glass
envelope was connected to the pipe at both ends by teflon
bushings. O-rings sealed the bushings with the glass
envelope and hose clamps held down the teflon bushings to
the pipe. Any minor air leaks encountered were sealed
with Gevac vacuum sealer. This arrangement does not allow
any power from the heater to escape into the atmosphere
since the pipe encloses the heater. Since the condenser
is also within the pipe, all of the heat going into the
condenser comes from the pipe. Since the temperature in
the annular space is only a few degrees higher than the

temperature in the vapor space, heat losses through the glass envelope are kept at a minimum. This makes it very easy to determine the heat fluxes into and out of the pipe.

As the evaporator heat flux was increased, the amount of liquid being vaporized also increased, causing the pressure in the vapor space to rise. It was not desirable, though, to have the pressure change when experiments were being performed. To correct this, a pressure adjuster designed by W. L. Mosteller [16] was connected to the system by a tap through the teflon bushing at the condenser end. It consisted of a piston-cylinder arrangement that enclosed a maximum volume of twenty-four cubic inches. When the pressure in the system began to rise, the piston was raised, and the increased volume forced the pressure back down. If the pressure was too low, the volume was decreased by lowering the piston. The pressure in the system was indicated by a bourdon tube, vacuum-pressure gage.

The choice of a wick material is very important in order to obtain good heat pipe operation. The capillary passages must be large enough to reduce the resistance to the liquid flow, yet small enough to provide adequate capillary pumping. In order to investigate the effect of wick parameters on the processes above, three mesh sizes of plain weave, nickel wire cloth were used: fifty by forty, eighty, and one-fifty mesh. Each type of mesh was applied by wrapping it tightly around the pipe until

a desired thickness was reached. Details of this procedure will be discussed in a later section.

The primary measurements made during the experiment were the temperatures along the surface of the pipe. This was done by placing five type-T, copper-constantan, metallic, sheathed thermocouples in milled grooves. The thermocouples were .041 inches O.D., and were silver soldered into the pipe in the positions indicated in Figure 2. The pipe was then machined to its original shape.

A .031 in. O.D. thermocouple, of the type described above, was used to measure the temperature in the vapor space. It was inserted through the bushing at the condenser end, and sealed so that it could traverse the length of the pipe. Other thermocouples were used in the condenser inlet, the condenser outlet, and the annular space in the glass envelope.

The thermocouples were referenced with a water-ice bath, and attached to a multi-connector plug. The plug was placed in an insulated metal box with a thermocouple selector switch on the outside. Readings, in millivolts, were made with a Hewlett-Packard 2010 Data Acquisition System, which included an integrating digital voltmeter and a guarded data amplifier.

Figure 4 is a block diagram of the entire system, and Figure 5 is a photograph of the apparatus.
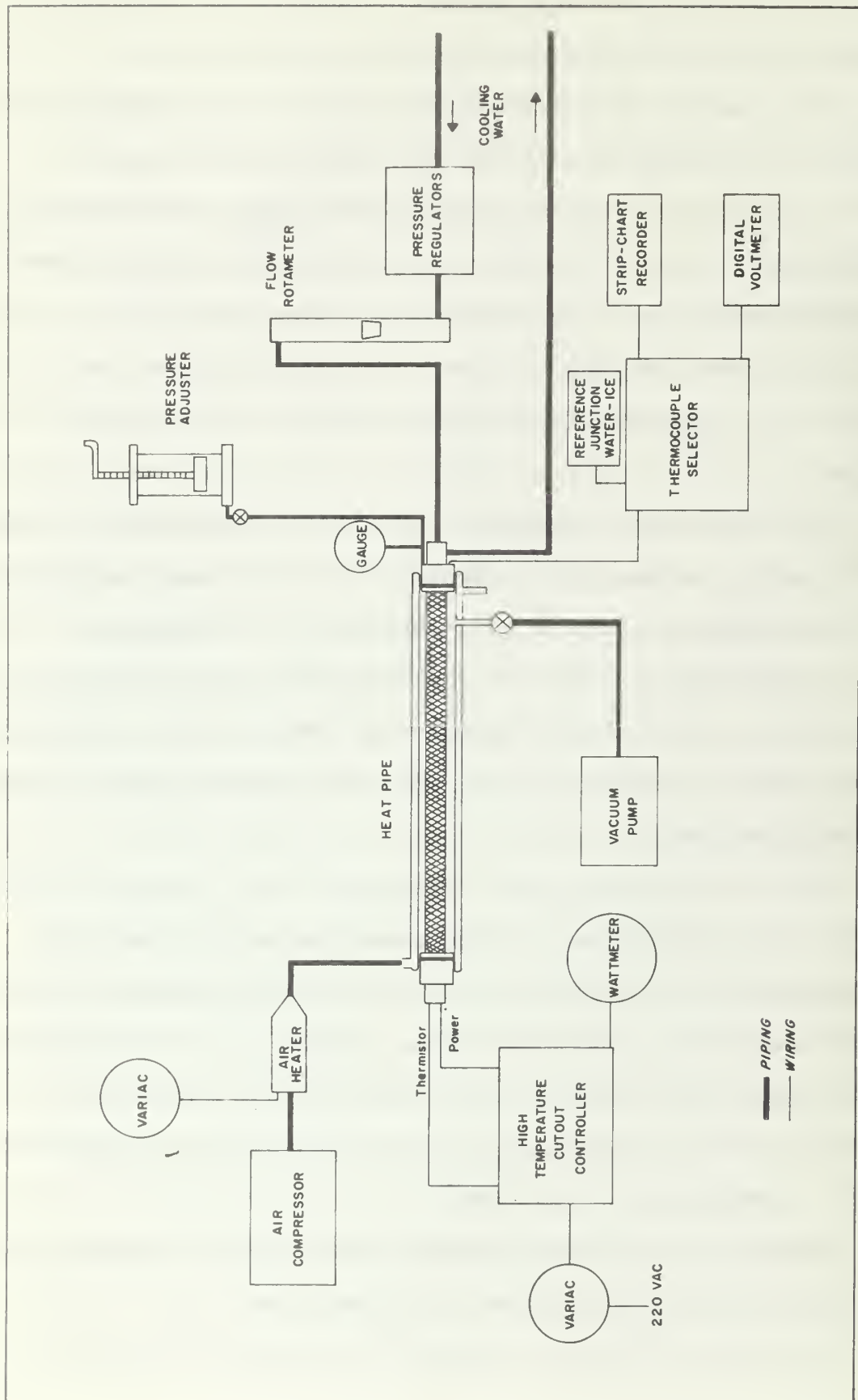
Fig. 4 Block Diagram of Heat Pipe Apparatus

24
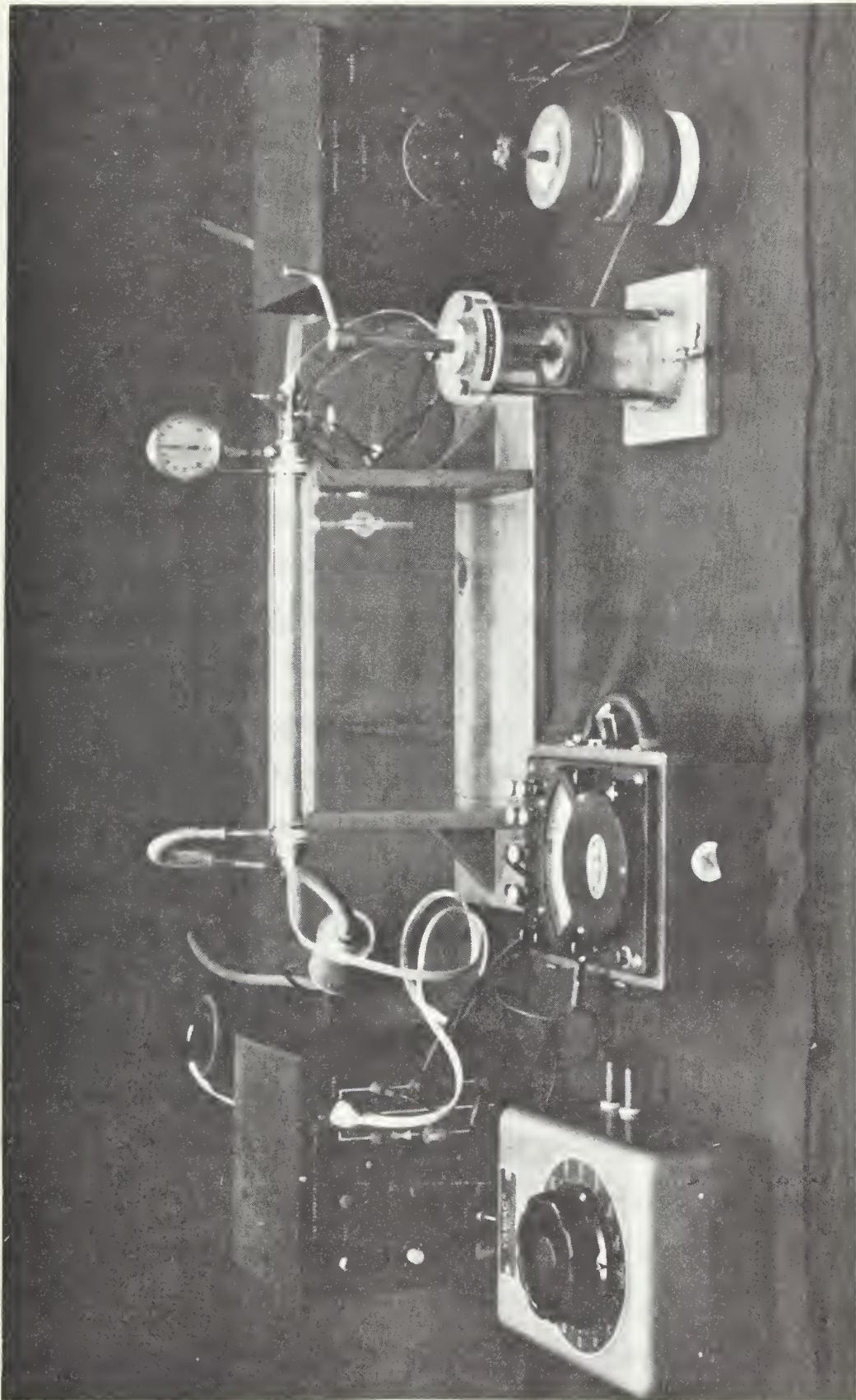
Figure 5. Photograph of Heat Pipe Apparatus

III. EXPERIMENTAL PROCEDURE

In an effort to minimize nucleate boiling, the heat pipe was smoothed with various grades of emery paper until a high polish was achieved. The pipe was then washed with a cleaning detergent, Alconox, followed by a rinsing with distilled water. This was necessary to be sure that the system was not contaminated, and to insure wettability of the pipe.

The first wire cloth applied to the pipe was the forty by fifty mesh. The ability of the working fluid to wet this cloth, and any other wicking material, is of extreme importance. Obviously, a wick that does not wet well will not have the capability of returning condensate to the evaporator. In order to enhance the wetting of the forty by fifty mesh, great care was taken in the preparation of the cloth. The cloth was first placed in a large, graduated cylinder along with a solution of hot water and Alconox. The graduated cylinder was then placed in an ultrasonic cleaner. After approximately one hour, the cloth was removed and washed in a solution of sulfuric acid, using a clean toothbrush to scrub the screen. The acid solution contained four parts of water and one part of 99.5% pure sulfuric acid (H_2SO_4). Seven or eight rinsings with distilled water followed. The next step in the procedure required the cloth to be rinsed in acetone,

and finally, to be washed completely with distilled water.
The handling of the screen, for the entire process, was
done using clean rubber gloves. When the screen was not
being washed, it was kept in a sealed glass jar which
prevented dust and other particles from fouling the cloth
surface.

Upon completion of the cleaning procedure, the cloth
was ready for application to the pipe. One edge of the
cloth was spot welded to the surface of the pipe; the
cloth was wound around the pipe to achieve a specified
wick thickness, and then the remaining edge was welded
down. The wick thickness in this case was .03 inches,
which for the fifty by forty mesh required two layers of
cloth. Two layers of cloth were then put on over the
original two to attain a wick thickness of .06 inches
followed by two more layers to reach the maximum wick
thickness of .10 inches. The outer layers were applied
to the pipe in the same manner as the first two. Extreme
care was taken to ensure that each succeeding edge of screen
was lined up with the previous one, in order to prevent
large discontinuities caused by overlapping.

The non-condensible gasses were then evacuated from
the system using a vacuum pump. When this was successfully
completed, an excess amount of working fluid was pumped
into the vapor space, using the pressure difference between
the atmosphere and the interior of the pipe as the driving
force. When the wick had become completely saturated,

the vacuum pump was used to pull the remaining fluid out.
A small amount of excess fluid was allowed to remain in
the bottom of the glass envelope, but was not allowed to
touch the wick.

Before applying power to the evaporator, the con-
denser, digital voltmeter, and air compressor were turned
on. The flow rate in the condenser varied from 1.75 to
2.15 gallons per minute, but this was observed to have no
effect on the rate of heat removal from the system. The
digital voltmeter had to be in operation for nearly one
hour before readings accurate to 1/1000 of a millivolt
could be made. The air compressor pumped the warm air
into the annulus of the envelope, allowing the glass to
warm up before the pipe was started.

In the initial stages of this investigation it was
noticed that even though the screen was thoroughly
cleaned, it would not transport water to the evaporator
when heat was first applied to the pipe. It appears that
there is an aging process involved when using a metal
wick which requires the wick to operate for several hours
before it becomes effective. This was accomplished by
operating the pipe at ten watts per square inch until
successive tests were made which produced the same dryout
point. The entire aging process was completed with the
full six layers and lasted approximately eight hours.

When the screen had been sufficiently aged, twenty
watts was the initial application of power to the evaporator.

28

The pressure was then adjusted to account for the increasing pressure within the system. When the system reached steady state, that is, the surface temperature of the pipe no longer increased, the nine thermocouple outputs were recorded. Power was then added in increments of twenty watts and the procedure was repeated. When power was applied to the evaporator the temperature at the surface of the pipe increased rapidly. When the surface temperature of the pipe did not level off, the power to the evaporator was discontinued. This is the condition reached when the wick had already attained its maximum capillary pumping rate and was not capable of providing more coolant to the evaporator. Many names have been applied to this condition, such as break - point, burnout point, and dryout point. Dryout point will be used in the remainder of this report.

The above procedure was used with operating pressures of 25 inches mercury vacuum, 10 inches mercury vacuum, and 5 pounds per square inch gage. When these tests were taken for both ethyl alcohol and water, the wick thickness was reduced to .06 inches by removing the outer two layers of screen. The screen on the pipe was then washed with the Alconox solution and scrubbed with a toothbrush. Several rinsings of distilled water, again using the toothbrush, completed the cleaning process. The pipe was then inserted back into the glass envelope, and the same tests were performed at the same pressures, with

the same fluids. The wick thickness was then reduced to
.03 inches, the screen was cleaned, and tests were per-
formed in the manner previously described. Upon completion
of these tests the eighty mesh cloth replaced the fifty
by forty mesh, and the exact procedure was repeated. The
procedure was repeated, finally, for the one-fifty mesh
cloth except that six layers of cloth were needed to
obtain a wick thickness of .03 inches.

IV. HEAT PIPE THEORY

Inside the heat pipe, the sum of the pressure changes throughout the system is equal to zero. That is,

$$[P_{L_e} - P_{V_e}] + [P_{V_e} - P_{V_c}] + [P_{V_c} - P_{L_c}] + [P_{L_c} - P_{L_e}] = 0 \quad (1)$$

where the terms of the equation are illustrated in Figure 6.

GLASS ENVELOPE
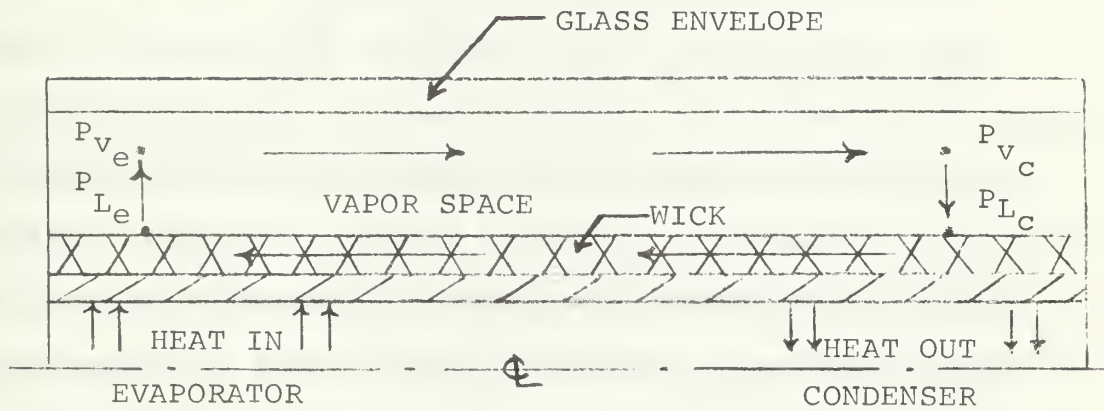
Figure 6. Schematic of Heat Pipe Flow Cycle

The first and third terms of equation (1) are the pressure drops across the liquid-vapor interfaces and can be expressed by the Laplace-Young equation of capillarity [1]. The first term becomes

$$P_{L_e} - P_{V_e} = \gamma \left(- \frac{2}{R_e}\right) \quad\quad\quad (2)$$

where γ is the surface tension of the working fluid, and R_e is the radius of curvature in the evaporator. The term

31

is negative since the direction of motion is from the wick surface to the vapor space. The third term in equation (1) is

$$P_{V_C} - P_{L_C} = \gamma \frac{2}{R_C} \tag{3}$$

where R_C is the radius of curvature in the condenser. The conbination of equations (1), (2), and (3) result in equation (4).

$$[P_{V_e} - P_{V_C}] + [P_{L_C} - P_{L_e}] = [\frac{2\gamma}{R_e}] - [\frac{2\gamma}{R_C}] \tag{4}$$

In a static condition the radius of curvature in the wick will be constant, that is, $R_e = R_C$. However, as heat is added to the system, the radius of curvature in the evaporator decreases since the liquid-vapor interface is receding into the wick. On the contrary, the radius of curvature in the condenser increases as liquid condenses on the wick. Thus, R_e will always be less than R_C. A limiting condition is reached when the capillary wick is operating at its maximum pumping rate. The smallest radius of curvature that is attained in the evaporator is R_{min}, while the radius of curvature in the condenser approaches infinity. R_{min} for wire cloth is given by $r_c/\cos \theta$ [14], where r_c is the characteristic pore radius of the wick and θ is the wetting angle between the fluid and the wick. With these substitutions equation (4) becomes

32

$$\Delta P_V - \Delta P_L = \frac{2 \gamma \cos \theta}{r_c} \tag{5}$$

where $\Delta P_x = P_{xe} - P_{xc}$. In this equation the equality sign characterizes the condition where the wick has attained its maximum pumping potential. This is also the limiting condition on the axial heat flux.

Equation (5) is valid for heat pipes in a variety of shapes and sizes. The individual terms on the left side of the equation, however, will vary according to the physical geometry of the pipe. In a conventional heat pipe the ΔP_V term in equation (5) is for vapor flow through a pipe, while the ΔP_L term is for liquid flow through an annulus. Since an everted heat pipe was used in this investigation, the ΔP_V term represents vapor flow through an annulus and the ΔP_L remains as liquid flow through an annulus. The vapor flow in an annulus is similar to annular flow with injection through a porous wall at the inner surface. Assuming laminar, incompressible flow, a Reynolds number is introduced, based on the injection velocity of the vapor leaving the wick [14].

$$N_{Rr} = \frac{1}{2 \pi \mu_V} \frac{d\dot{m}}{dz} \tag{6}$$

where $\dot{m}_V$ is the vapor mass flow rate, z is the axial direction of the pipe, and μ_V is the viscosity of the vapor. When $|N_{Rr}| \ll 1$ the vapor pressure gradient becomes that for steady, laminar flow [14]. For an annulus this is given by [Appendix A]

33

$$\frac{dP_v}{dz} = -\frac{\dot{m}_v 8\mu_v}{\pi \rho_v} \left[\frac{1}{r_g^4 - r_o^4 - \dfrac{(r_g^2 - r_o^2)^2}{\ln r_o/r_g}} \right] \tag{7}$$

where ρ_v is the density of the vapor,

   r_i is the radius of the wick-pipe interface,

   r_o is the outer radius of the wick,

and r_g is the inner radius of the glass envelope.

These terms are illustrated in Figure 7.
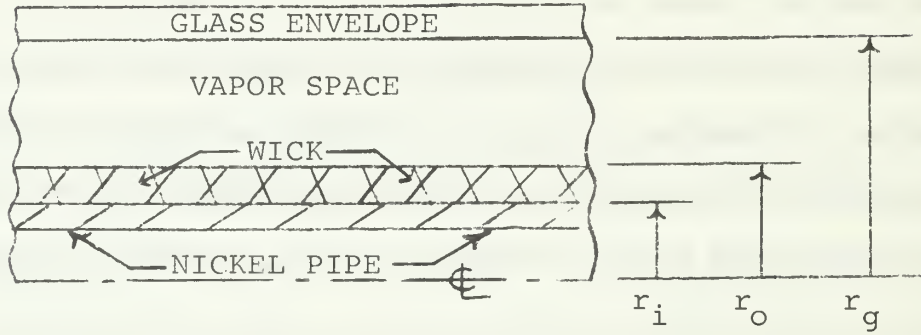
Figure 7.   Cross-Section of Everted Heat Pipe

When there is constant heat addition in the evaporator, and removal in the condenser, then

$$\dot{m}_v(z) = \frac{z}{L_e} \frac{Q_e}{\lambda} \qquad 0 \le z \le L_e$$

$$\dot{m}_v(z) = \frac{L-z}{L-L_e} \frac{Q_e}{\lambda} \quad L_e \le z \le L \tag{8}$$

34

where Q_e is the heat into the evaporator,

    L is the length of the pipe,

    L_e is the length of the evaporator section

and λ is the latent heat of vaporization of the working fluid.

Combining equations (7) and (8) and integrating from 0 to L yields

$$\Delta P_v = \frac{4 Q_e \mu_v L}{\pi \rho_v \lambda} \left[\frac{1}{r_g^4 - r_o^4 - \frac{(r_g^2 - r_o^2)^2}{\ln\, r_o/r_g}} \right] \tag{9}$$

When $|N_{Rr}| \gg 1$ the pressure gradient for flow in a pipe is represented by [14]

$$\frac{dP_v}{dz} = \frac{-s\, \dot{m}_v}{\pi \rho_v r_v^4} \quad \frac{d\dot{m}_v}{dz} \tag{10}$$

where s equals 1 for evaporation, $\pi/4$ for condensation,

and r_v is the radius of the vapor space in a pipe.

It will be assumed in this analysis that the flow properties in an annulus will be given by

$$\frac{dP_v}{dz} = \frac{-s\dot{m}_v}{\pi \rho_v} \quad \frac{d\dot{m}_v}{dz} \left[\frac{1}{r_g^4 - r_o^4 - \frac{(r_g^2 - r_o^2)^2}{\ln\, r_o/r_g}} \right] \tag{11}$$

By making use of equation (8) and integrating from 0 to L, equation (11) becomes

$$\Delta P_v = \frac{(1 - 4/\pi^2) Q_e^2 \, \mu_v}{8\rho_v \, \lambda^2} \left[\frac{1}{r_g^4 - r_o^4 - \dfrac{(r_g^2 - r_o^2)^2}{\ln r_o/r_g}} \right] \tag{12}$$

The equation which describes the liquid flowing through the annular wick, a form of Darcy's law [17], is

$$\frac{dP_L}{dz} = \frac{\mu_f \, \dot{m}_f}{\pi (r_o^2 - r_i^2) \rho_f N_m} \tag{13}$$

N_m is a friction term that is the inverse of the wick permeability. The permeability is defined as the ease with which a fluid can pass through the wick. For a homogeneous, porous wick [14]

$$N_m = \frac{\varepsilon r_c^2}{b} \tag{14}$$

where ε is the fraction of wick volume occupied by liquid, and b is a dimensionless constant.

Integrating equation (13) from 0 to L yields the pressure drop in the wick.

$$\Delta P_L = \frac{-b \, \mu_f \, Q_e \, L}{2\pi (r_o^2 - r_i^2) \rho_f \lambda \varepsilon r_c^2} \tag{15}$$

Combining equations (5), (9), (15) and (5), (12), (15) results in equations (16) and (17), which together describe the system.

36

$$\frac{4Q_e \mu_v L}{\pi \rho_v \lambda} \left[\frac{1}{r_g{}^4 - r_o{}^4 - \frac{(r_g{}^2 - r_o{}^2)^2}{\ln r_o/r_g}} \right] + \frac{b\mu_f Q_e L}{2\pi(r_o{}^2 - r_i{}^2)\rho_f \lambda \varepsilon r_c{}^2} \leq \frac{2\gamma \cos\theta}{r_c} \quad (16)$$

$$\frac{(1 - 4/\pi^2)Q_e{}^2}{8\rho_v \lambda^2} \left[\frac{1}{r_g{}^4 - r_o{}^4 - \frac{(r_g{}^2 - r_o{}^2)^2}{\ln r_o/r_g}} \right] + \frac{b\mu_f Q_e L}{2\pi(r_o{}^2 - r_i{}^2)\rho_f \lambda \varepsilon r_c{}^2} \leq \frac{2\gamma \cos\theta}{r_c} \quad (17)$$

The evaporator heat flux in equation (16) is a function of the working fluid, the wick material, and the dimensions of the pipe. When a given fluid is used in the pipe, the terms θ, μ, ρ, λ, and γ become fixed, assuming constant pressure and temperature. For a given wick, ε and b will become fixed values. The terms r_g, r_i, and L are fixed by the dimensions of the pipe. Assuming that r_o is an unknown constant, equation (16) can be written in the form

$$A\,Q_e + BQ_e/r_c{}^2 = \frac{C}{r_c} \quad (18)$$

where $A = \dfrac{4\mu_v L}{\pi \rho_v \lambda} \left[\dfrac{1}{r_g{}^4 - r_o{}^4 - \dfrac{(r_g{}^2 - r_o{}^2)^2}{\ln r_o/r_g}} \right]$

$$B = \frac{b\mu_f L}{2\pi(r_o{}^2 - r_i{}^2)\rho_f \lambda \varepsilon}$$

and $C = 2\gamma \cos\theta$

Q_e is now only dependent on r_c. The value of r_c that

maximizes Q_e was determined by setting the derivative of Q_e, with respect to r_c, equal to zero. Therefore,

$$(r_c)_{opt} = (\frac{B}{A})^{\frac{1}{2}}$$

(19)

or

$$(r_c)_{opt} = \left[\frac{b\mu_f\rho_v}{8\epsilon\mu_v\rho_f} \frac{r_g^4 - r_o^4 - \frac{(r_g^2 - r_o^2)^2}{\ell n\ r_o/r_g}}{r_o^2 - r_i^2} \right]^{\frac{1}{2}}$$

(20)

Equation (20) is an expression for the value of r_c which will allow maximum heat transport in the pipe when all other values are constant. Substituting equation (19) into equation (18) yields an expression for Q_e.

$$Q_e = \frac{C}{2(AB)^{\frac{1}{2}}}$$

(21)

or

$$Q_e = 2\gamma\cos\theta \left[\frac{\pi^2\epsilon\rho_f\rho_v\lambda^2(r_o^2 - r_i^2)\left[r_g^4 - r_o^4 - \frac{(r_g^2 - r_o^2)^2}{\ell n\ r_o/r_g}\right]}{2\mu_v\mu_f bL^2} \right]^{\frac{1}{2}}$$

(22)

It is clear from equation (22) that Q_e is dependent on the value of r_o, the outer radius of the screen. Q_e will be maximum when the term

$$[r_o^2 - r_i^2]\left[r_g^4 - r_o^4 - \frac{(r_g^2 - r_o^2)^2}{\ell n\ r_o/r_g}\right]$$

(23)

38

has its largest value. The only unknown in expression (23) is r_o, as r_i equals .375 inches and r_g equals .670 inches. If the derivative of expression (23) is taken with respect to r_o, and set equal to zero, an optimal value for r_o can be obtained. Thus

$$\frac{(r_o{}^2-r_i{}^2)\,[-4r_o{}^3-4r_o\ln(\frac{r_o}{r_g})\,(r_g{}^2-r_o{}^2)+\frac{r_g}{r_o}(r_g{}^2-r_o{}^2)^2]}{2[(r_o{}^2-r_i{}^2)\,(r_g{}^4-r_o{}^4+(r_g{}^2-r_o{}^2)^2\,\ln\frac{r_o}{r_g})]^{\frac{1}{2}}} +$$

$$\frac{2r_o\,[r_g{}^4-r_o{}^4+(r_g{}^2-r_o{}^2)^2\,\ln\frac{r_o}{r_g}]}{2[(r_o{}^2-r_i{}^2)\,(r_g{}^4-r_o{}^4+(r_g{}^2-r_o{}^2)^2\,\ln\frac{r_o}{r_g})]^{\frac{1}{2}}} = 0 \qquad (24)$$

Using the numerical values of r_i and r_g, equation (24) was iteratively solved to give an optimum value of r_o equal to .561 inches. If the radius of the pipe, .375 inches, is then subtracted from r_o the optimum wick thickness is .186 inches. This means that the heat pipe, when characterized by equation (16), can transfer the most heat when a value of r_c given by equation (19) is used in conjunction with a wick thickness of .186 inches.

The same procedure for finding the maximum heat transfer was then used on equation (17). Assuming that all variables except r_c are constants, equation (17) is given by

$$DQ_e{}^2 + BQ_e/r_c{}^2 = \frac{C}{r_c} \qquad (25)$$

where $D = \dfrac{1 - 4/\pi^2}{8 \, \rho_v \, \lambda^2} \left[\dfrac{1}{r_g^{\,4} - r_o^{\,4} - \dfrac{(r_g^2 - r_o^2)^2}{\ell n \; r_o/r_g}} \right]$

The value of r_c that would maximize Q_e is found by setting the derivative of Q_e with respect to r_c equal to zero, yielding

$$(r_c)_{opt} = [\frac{2B^2}{DC}]^{1/3} \tag{26}$$

or

$$(r_c)_{opt} = \left[\dfrac{2b^2 \mu_f^{\,2} L^2 \rho_v [r_g^{\,4} - r_o^{\,4} - \dfrac{(r_g^{\,2} - r_o^{\,2})^2}{\ell n \; r_o/r_g}]}{(\pi^2 - 4) \, \gamma \cos \theta \, (r_o^{\,2} - r_i^{\,2}) \rho_f^{\,2} \epsilon^2} \right]^{1/3} \tag{27}$$

Substituting equation (26) into equation (25) gives the following expression:

$$Q_e = \dfrac{B}{A \, r_c^{\,2}} \tag{28}$$

or

$$Q_e = \pi\lambda \left[\dfrac{16\rho_v \rho_f \epsilon \gamma^2 (\cos\theta)^2 (r_o^{\,2} - r_i^{\,2}) [r_g^{\,4} - r_o^{\,4} - \dfrac{(r_g^{\,2} - r_o^{\,2})^2}{\ell n \; r_o/r_g}]}{b \mu_f L \, (\pi^2 - 4)} \right]^{1/3} \tag{29}$$

However, the magnitude of Q_e is still dependent on the value of r_o. The heat transfer will reach a maximum when the term

40

$$[r_o^2 - r_i^2] \left[r_g^4 - r_o^4 - \frac{(r_g^2 - r_o^2)^2}{\ln r_o/r_g} \right] \qquad (30)$$

reaches its highest value. This was just shown to be the case when r_o equals .186 inches. The maximum heat transport for equation (17) is reached when the wick thickness is .186 inches, and the value of r_c is given by equation (26).

V.   DISCUSSION OF RESULTS

Data was obtained in this study by operating the heat pipe with various combinations of two fluids, three pressures, and three mesh sizes of plain weave, nickel, wire cloth. A total of fifty-four tests were made, and the parameters for each test are described in Table 1. Each test was stopped when the dryout point was reached. This is the condition where the maximum capillary pumping rate and the maximum heat transfer rate, Q_e, exist. Experimental values of Q_e are also listed in Table 1.

In low temperature heat pipes the vapor pressure is a small part of the total pressure loss and can be neglected when compared to the pressure in the wick [18, 19]. This was true for the heat pipe considered in this study. Equations (16) and (17), neglecting the vapor pressure drop, may be simplified to give

$$\frac{b \mu_f L \, Q_e}{2\pi (r_o^2 - r_i^2) \rho_f \lambda \varepsilon r_c^2} = \frac{2 \gamma \cos \theta}{r_c} \tag{31}$$

The maximum heat transfer rate that the heat pipe can maintain occurs when the liquid flow rate is maximum, and is found by rearranging equation (31) to get

$$\overset{\text{(I)}}{} \quad \overset{\text{(II)}}{} \quad \overset{\text{(III)}}{} \quad \overset{\text{(IV)}}{}$$

$$Q_e = [4\pi(r_o^2 - r_i^2)] \quad [\frac{\rho_f \lambda \gamma}{\mu_f}] \quad [\frac{\cos \theta}{L}] \quad [\frac{\varepsilon \, r_c}{b}] \tag{32}$$

TABLE 1

Summary of Test Parameters

Test	Mesh Size	Wick Thickness	Pressure	Fluid	Dryout (watts/in^2)
1	50	.096	25 in. Hg	water	20
2	50	.096	10 in. Hg	water	-
3	50	.096	5 psi	water	-
4	50	.096	25	alcohol	12
5	50	.096	10	alcohol	16
6	50	.096	5	alcohol	20
7	50	.064	25	water	24
8	50	.064	10	water	44
9	50	.064	5	water	-
10	50	.064	25	alcohol	12
11	50	.064	10	alcohol	16
12	50	.064	5	alcohol	20
13	50	.032	25	water	26
14	50	.032	10	water	30
15	50	.032	5	water	34
16	50	.032	25	alcohol	8
17	50	.032	10	alcohol	10
18	50	.032	5	alcohol	12
19	80	.112	25	water	12
20	80	.112	10	water	18
21	80	.112	5	water	24
22	80	.112	25	alcohol	4
23	80	.112	10	alcohol	10
24	80	.112	5	alcohol	12
25	80	.056	25	water	12
26	80	.056	10	water	18
27	80	.056	5	water	22
28	80	.056	25	alcohol	6
29	80	.056	10	alcohol	10

TABLE 1 (Continued)

Test	Mesh Size	Wick Thickness	Pressure	Fluid	Dryout (watts/in^2)
30	80	.056	5	alcohol	12
31	80	.028	25	water	10
32	80	.028	10	water	16
33	80	.028	5	water	22
34	80	.028	25	alcohol	4
35	80	.028	10	alcohol	6
36	80	.028	5	alcohol	8
37	150	.105	25	water	12
38	150	.105	10	water	16
39	150	.105	5	water	24
40	150	.105	25	alcohol	6
41	150	.105	10	alcohol	10
42	150	.105	5	alcohol	12
43	150	.060	25	water	12
44	150	.060	10	water	16
45	150	.060	5	water	20
46	150	.060	25	alcohol	4
47	150	.060	10	alcohol	8
48	150	.060	5	alcohol	12
49	150	.030	25	water	12
50	150	.030	10	water	16
51	150	.030	5	water	18
52	150	.030	25	alcohol	4
53	150	.030	10	alcohol	8
54	150	.030	5	alcohol	10

Equation (32) shows that Q_e is a product of four factors.
The first factor, (I), is a function of the wick thickness;
the second, (II), is a grouping of the working fluid
properties; the third (III), is a function of the liquid-
wick interaction, and the fourth (IV), is a grouping of
the wick properties. When choosing a wick and a working
fluid these groupings should be kept as large as possible.
Representative experimental results have been plotted
and will be used in this discussion to explain how each
of the above parameters influences the heat transfer
capabilities of the pipe.

The term $\pi(r_o^2 - r_i^2)$ represents the annular area of
the wick that is available for fluid flow. As heat was
added to the evaporator the liquid level was observed to
recede into the wick, exposing the upper layers of the
wick to vapor. If the temperature of the upper layers
then became the temperature of the vapor, the outer wick
radius was effectively reduced to a value r_o' and the
effective annular area of the wick also decreased. Thus,
the term appearing in group (I) should not be the actual
annular area but an effective annular area, and its value
can only be approximated. As the effective area became
smaller, the impedance to the return flow grew larger.
Eventually, the flow was hindered so much that it could
not provide the evaporator with enough cooling fluid, and
evaporator dryout resulted. Figure 8 is a plot of the
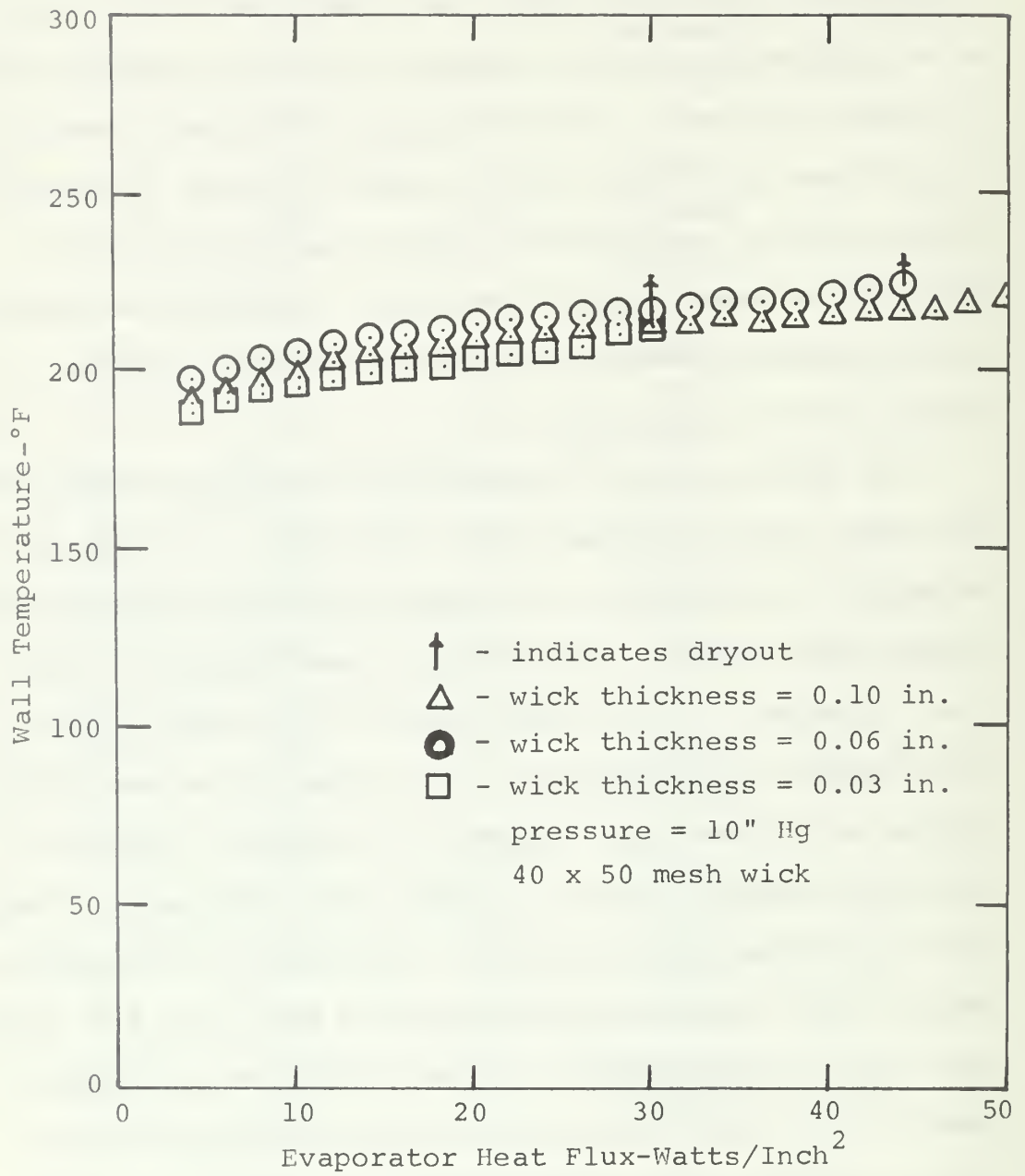heat flux versus the wall temperature as the actual wick

45

Figure 8. Heat Flux vs. Temperature for Water

thickness was decreased. When a wick thickness of .10 inches was used the pipe was still operating normally at fifty watts per square inch, the maximum available heat input. As the thickness was decreased the dryout point also decreased. Dryout occurred at forty-four and thirty watts per square inch, using wick thicknesses of .06 inches and .03 inches. Thus, it was experimentally determined that as the wick thickness was increased, the heat transfer rate at dryout also increased, in accordance with equation (32). This trend should increase until a wick thickness of .186 inches is reached. This was the optimum wick thickness arrived at by solving equation (24). The maximum heat transfer rate should decrease if the wick thickness is increased beyond .186 inches.

The terms appearing in group (II) are all properties of the working fluid. The liquid density, heat of vaporization, surface tension, and viscosity are all known values. It is evident that the best heat pipe fluids will have high densities, latent heat of vaporizations, and surface tensions, while the viscosity should be kept low. It is convenient to combine these terms into a single term, N_f, given by

$$N_f = \frac{\gamma \, \rho_f \, \lambda}{\mu_f} \tag{33}$$

This term has been calculated for a variety of possible working fluids at the Lewis Research Center [12]. In order

to determine the effect of fluid properties on heat pipe operation, two fluids were tested. Ethyl alcohol and distilled water were chosen since they were readily available and their values of N_f were quite different. At 70°F, N_f, in BTU-HR-LBF/FT^3, takes on a value of 138 for water and 9.9 for alcohol. By forming a ratio of these values it seems that water should be able to transfer almost thirteen times as much heat as ethyl alcohol. As will be shown in the next section, however, this is not the case.

The two terms appearing in group (III) are the wetting angle, θ, and the pipe length, L. These are both functions of the liquid-wick combination. If wicks of different material were being tested, such as fiberglass or packed beads, then the wetting angle would change with every test. In this study, however, three mesh sizes of the same type of wick were used. Thus, the wetting angle on the nickel was considered to be mainly a function of the working fluid, and not the mesh size of the screen. When the liquid saturates the wick a complicated matrix results, where the wetting angle is not well defined. Ethyl alcohol wets the wick much more readily than water, so it can be assumed that the ethyl alcohol had a lower wetting angle. This makes the value of $\cos(\theta)$ lower for water than for alcohol. However, nothing can be said about the precise numerical values of these wetting angles.

The value of L in equation (32) would be the actual
pipe length assuming that all fourteen inches of the
evaporator and condenser were utilized when the pipe was
in operation. As it turns out, though, the condenser was
overdesigned for this system, and only a fraction of the
condenser length was used during the experimentation.
Most of the condensing activity took place at the end
of the condenser nearest the evaporator. The activity
in the condenser decreased, as the distance from the
evaporator increased. It is obvious that some effective
length, L_{eff}, should be used in equation (32), but
assigning a value to it would only be an approximation.
This value is also a function of the working fluid and the
wick, but since the wicks in this study were all plain
weave, nickel, wire cloth, L_{eff} is assumed to be a function
of the working fluid only. It was noticed in all tests
that the effective length of the pipe was longer for water
than for alcohol. The effective length was observed to
increase slightly for both water and ethyl alcohol as the
heat flux was increased. Since cos θ is bigger and L_{eff} is
smaller for alcohol, the term cos θ/L_{eff} will be larger
for alcohol than for water. Thus, the effect of group
(III) in equation (32) is to yield a higher Q_e for ethyl
alcohol than water. This will diminish the effect of the
higher group (II) for water. Figure 9 illustrates the
experimental heat transfer rates of the two fluids.
Evaporator dryout occurred at forty-four watts per square
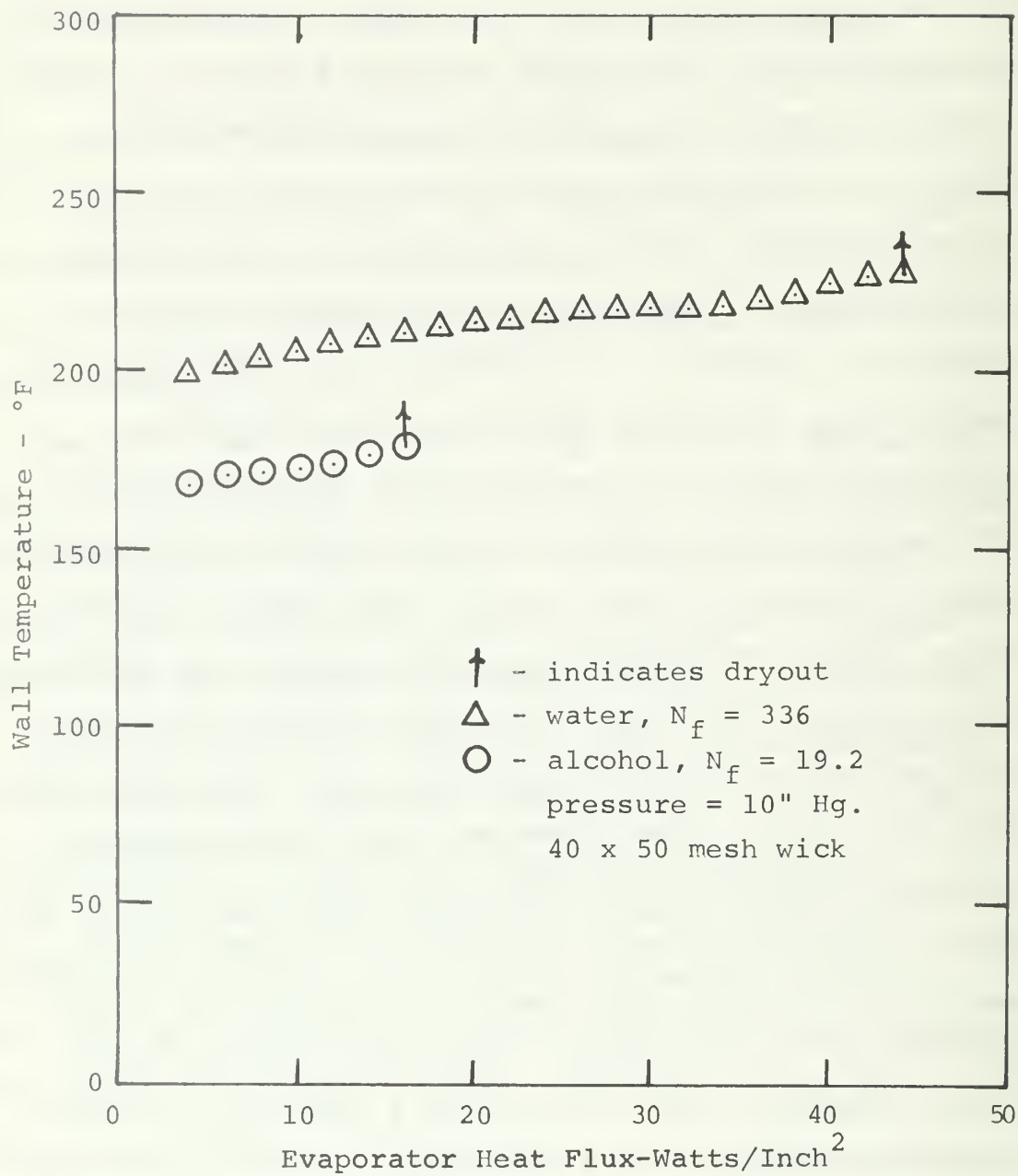inch when water was the working fluid, and sixteen watts

Figure 9. Heat Flux vs. Temperature

per square inch when ethyl alcohol was used. Experimentally speaking, then, water transferred two and three-quarters times more heat than did the ethyl alcohol.

The fourth group in equation (32) is a function of the wick properties. The porosity, ϵ, is defined as the percent of wick volume occupied by the liquid. Its value for the three types of mesh is presented in Table 2, along with other wick parameters. Sample calculations for these wick parameters appear in Appendix B. The porosity of the fifty mesh screen is approximately equal to that of the one-fifty mesh, but the porosity of the eighty mesh is much lower, tending to lower maximum heat transfer.

The capillary radius of the wick, r_c, should be large so that there is less resistance to the fluid flow, but small so that the capillary pumping is enhanced. The capillary radius is defined as a measure of the openings in the wick that the liquid uses to pull itself along. When the screen is wrapped in layers, a complicated wire matrix is formed. As the liquid returns to the evaporator it follows a tortuous path radially, through the screen, and axially, between the layers of screen. Defining r_c as half of the space opening in the screen would only take into account the flow through the layers. When layers of screen are stacked on each other, the screen with the thickest wires creates the largest gaps between layers. It is logical to assume, then, that a wick composed of thick

51

TABLE 2

Summary of Mesh Constants

	40x50 Mesh	80x80 Mesh	150x150 Mesh
Wire Diameter (inches)	.009	.007	.0026
Stacking Factor	1.78	2.00	1.54
Porosity (percent)	64.4	55.2	68.2
Surface Open Area (percent)	35.3	19.4	37.4
Space Opening (inches)	.0134*	.0055	.0041

* average

wire and large openings has a higher value for r_c than a wick with smaller dimensions. The fifty mesh screen has a space opening almost three times the size of the space openings in the other two screens. The wire diameter for the fifty mesh screen is slightly bigger than that for the eighty mesh screen, but three times as big for the wire in the one-fifty mesh screen. This indicates that the value of r_c for the fifty mesh screen is larger than that for the other two mesh sizes.

The third term in group (IV) is b, a dimensionless constant directly related to the permeability. For capillary structures with tortuous and interconnected pores the value of b lies between ten and twenty [14]. Exact values of b cannot be specified unless rigorous permeability tests are performed, such as those completed at the Lewis Research Center [12]. However, since b is directly proportional to the ease with which a fluid may pass through a wick, then a wick with the largest openings and the most open surface area should have the largest value for b. The eighty mesh screen only has nineteen percent of its surface area open, compared to thirty-five and thirty-seven percent for the fifty and one-fifty meshes. Also, the fifty mesh screen has a large space opening compared to the other two. This indicates a higher value for b for the fifty mesh screen than for the eighty or one-fifty mesh. Since the range of b is only from ten to twenty, the value for b for the fifty mesh screen can, at most, be twice that

53

of the other two screens. Assuming that the value of r_c is, at least, twice as big as the fifty mesh screen than for the eighty or one-fifty meshes, then $\varepsilon r_c/b$ will be largest for the fifty mesh screen. It is difficult to determine any difference in the magnitudes of $\varepsilon r_c/b$ for the eighty and one-fifty mesh screens since they have offsetting dimensions. The data plotted in Figure 10 shows that the eighty and one-fifty mesh screens reached dryout at the same heat flux, twenty watts per square inch. The fifty mesh screen continued to operate, until a heat flux of thirty-four watts per square inch was attained. Thus, the experimental results are in agreement with the predictions obtained by analyzing group (IV).

A very interesting feature of the system was the pressure controller. It enabled all data to be taken at constant pressures, and at the same time controlled the operating temperature within the pipe. When the operating temperature of the pipe was decreased the value of N_f was also decreased. Therefore, the maximum heat transfer, Q_e, will decrease as the pressure decreases. Figure 11 is a plot of the evaporator heat flux versus the wall temperature for three different pressures. As predicted, Q_e had its largest value at five pounds per square inch, and its lowest value at twenty-five inches Hg.

All of the data from the fifty four tests appears in Figures 12 through 17. The graphs presented in the discussion are representative of the data with one exception.
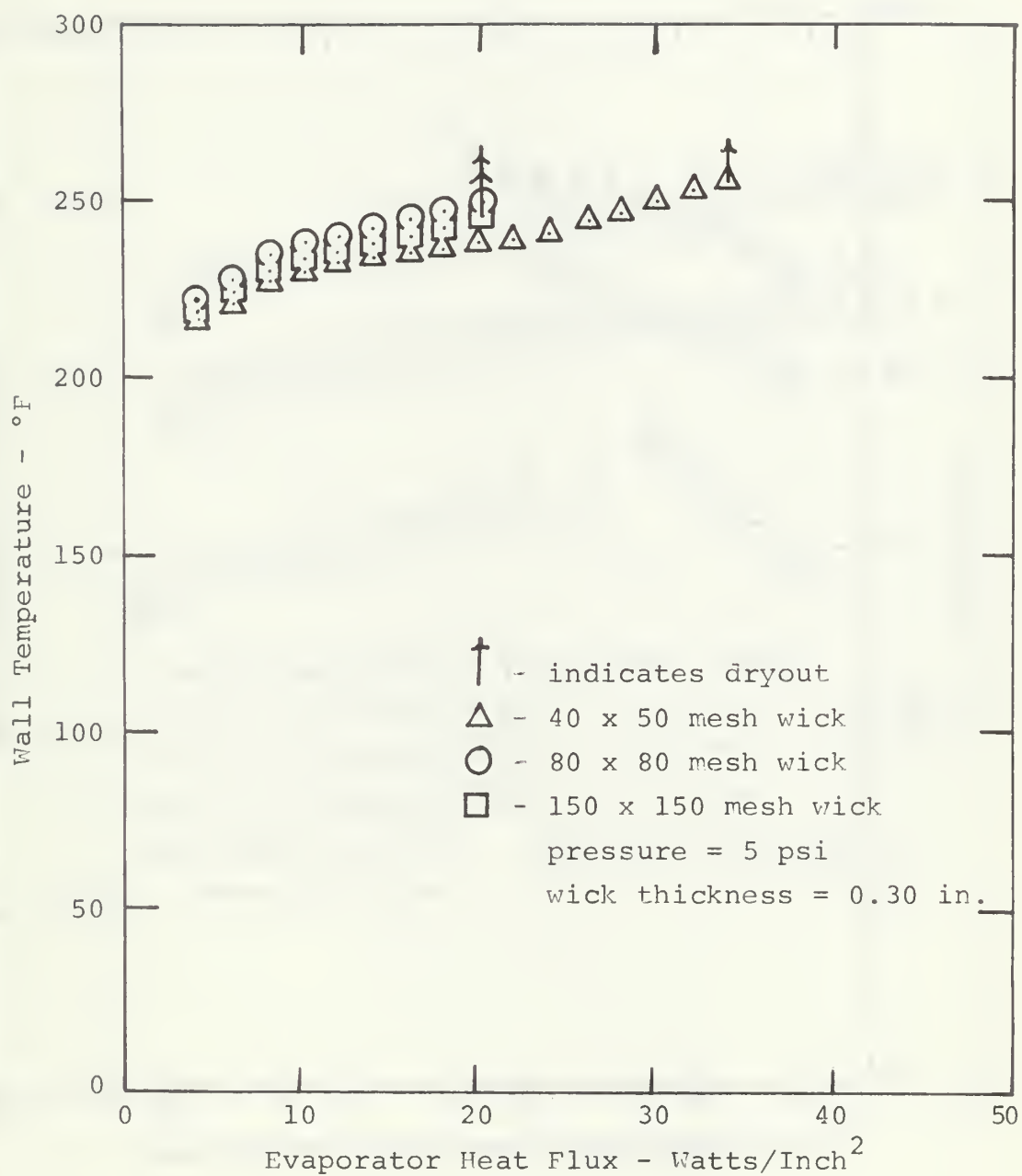
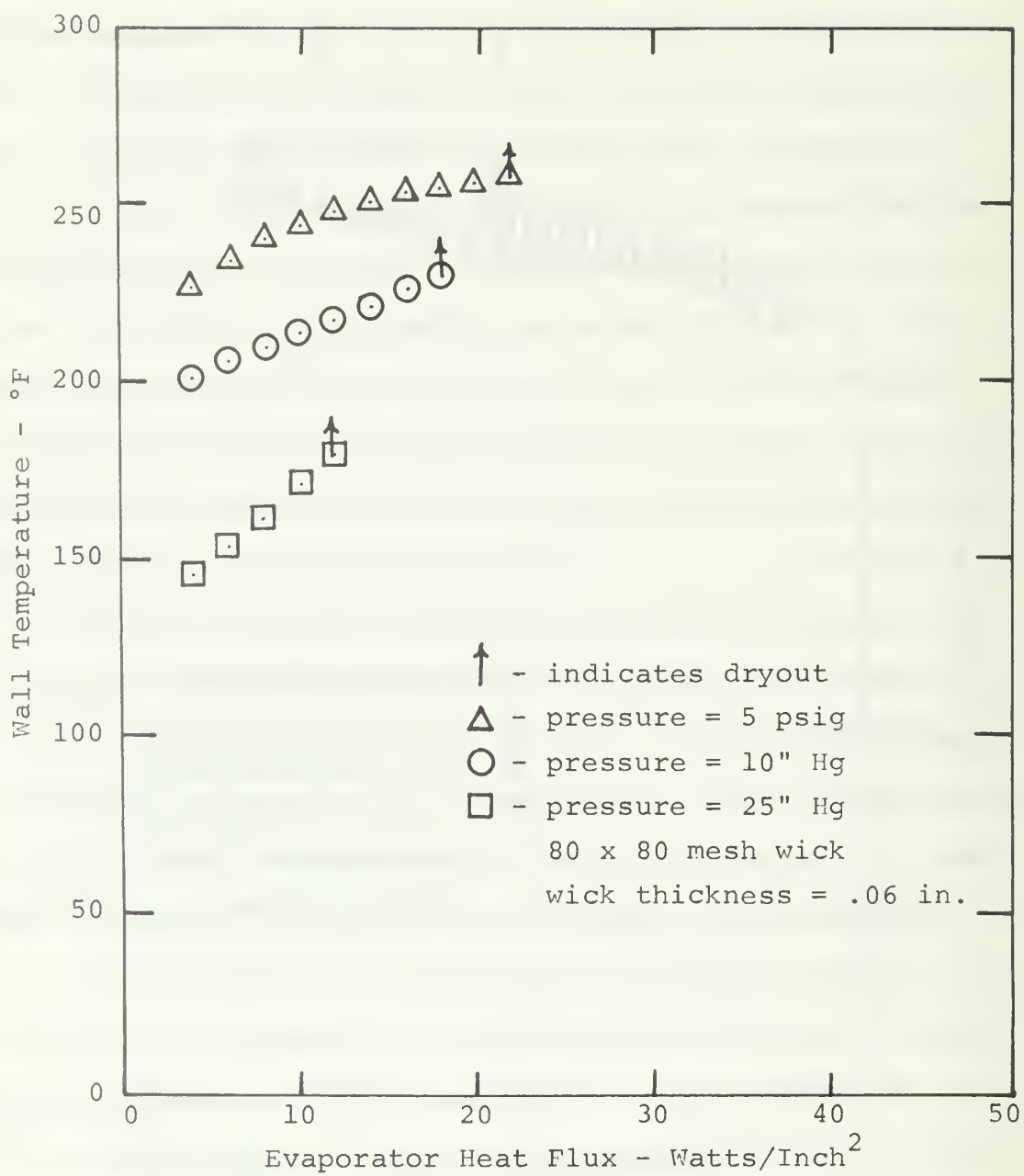Figure 10. Heat Flux vs. Temperature for Water

55

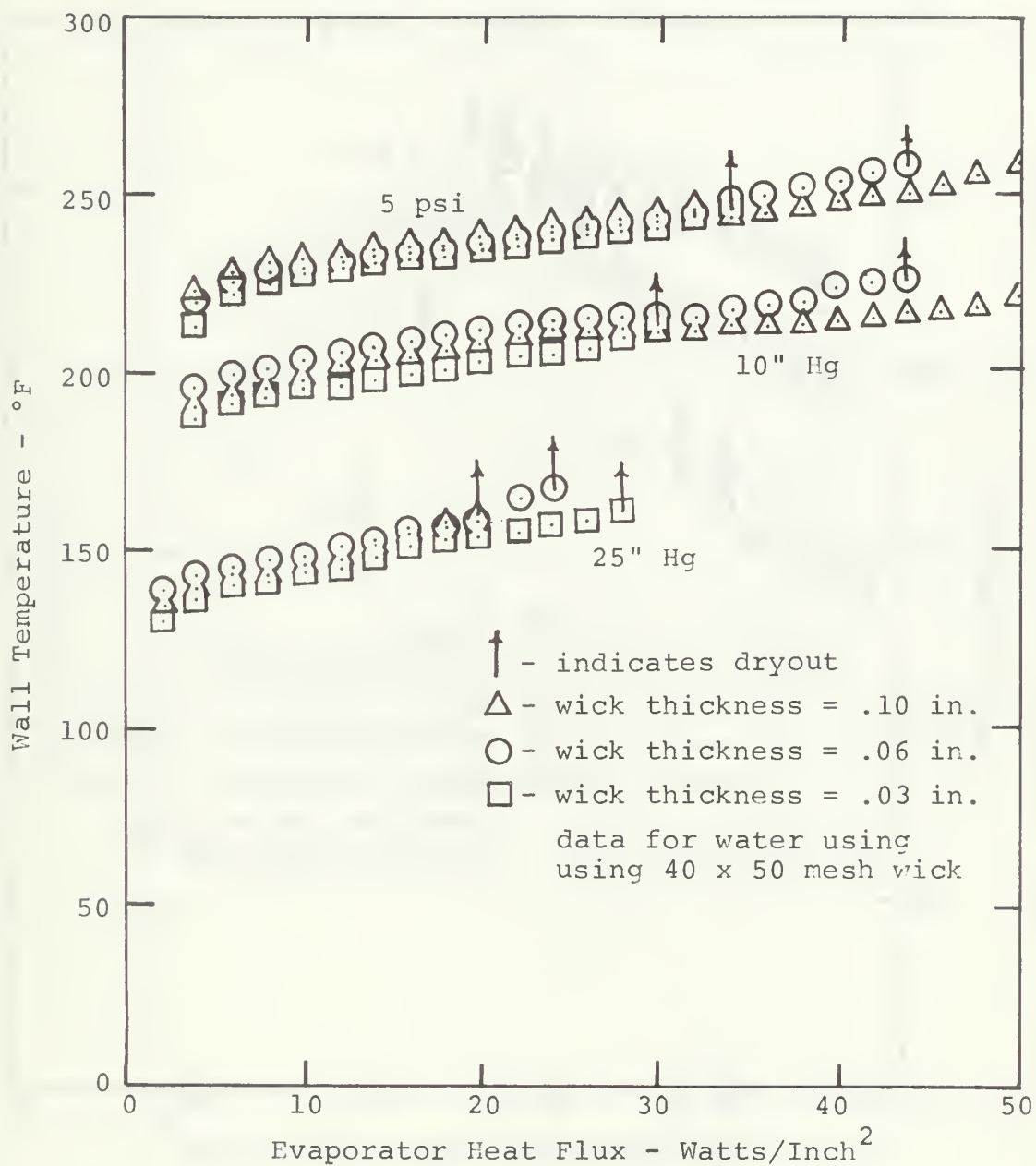Figure 11. Heat Flux vs. Temperature for Water

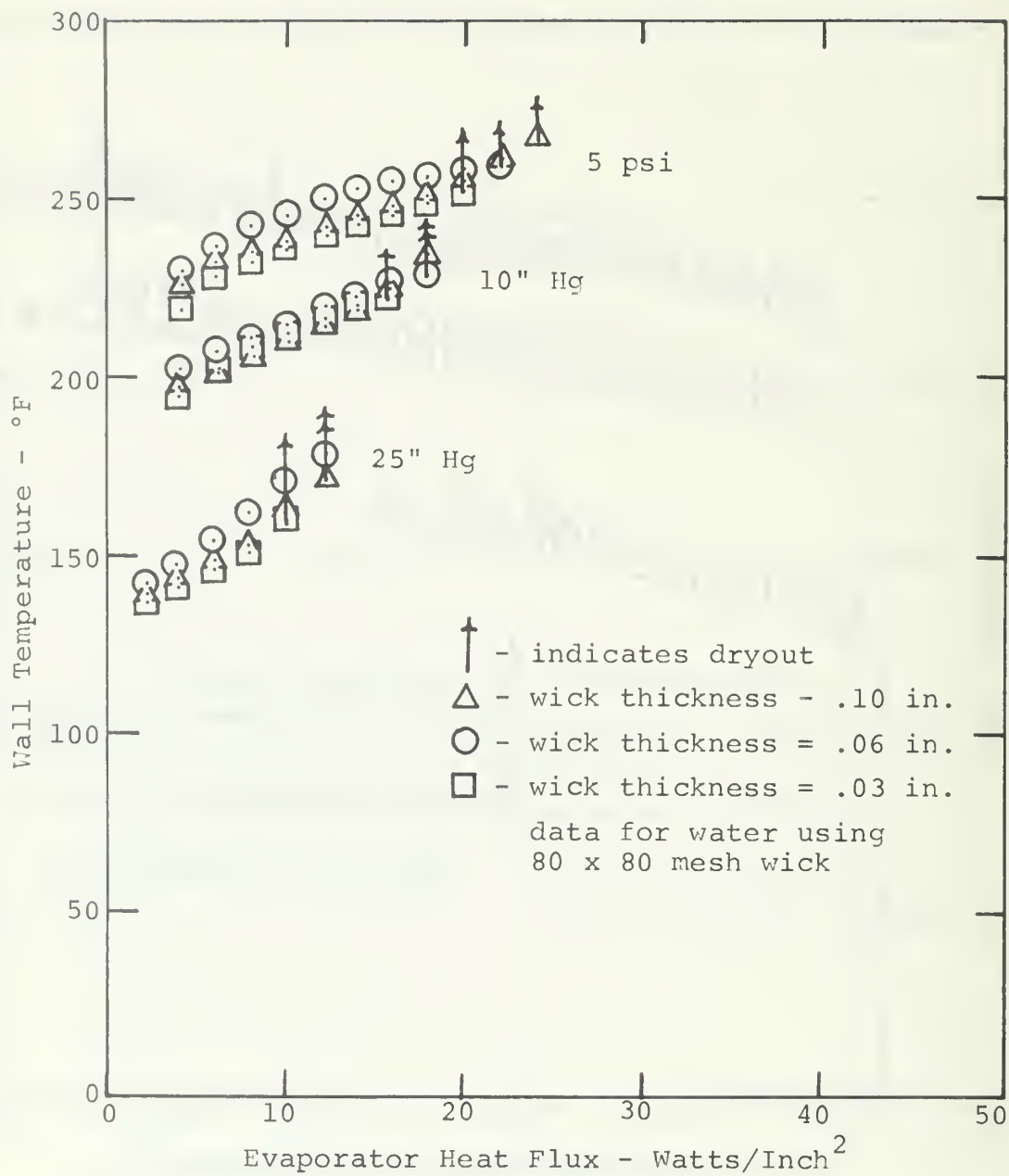Figure 12. Heat Flux vs. Temperature
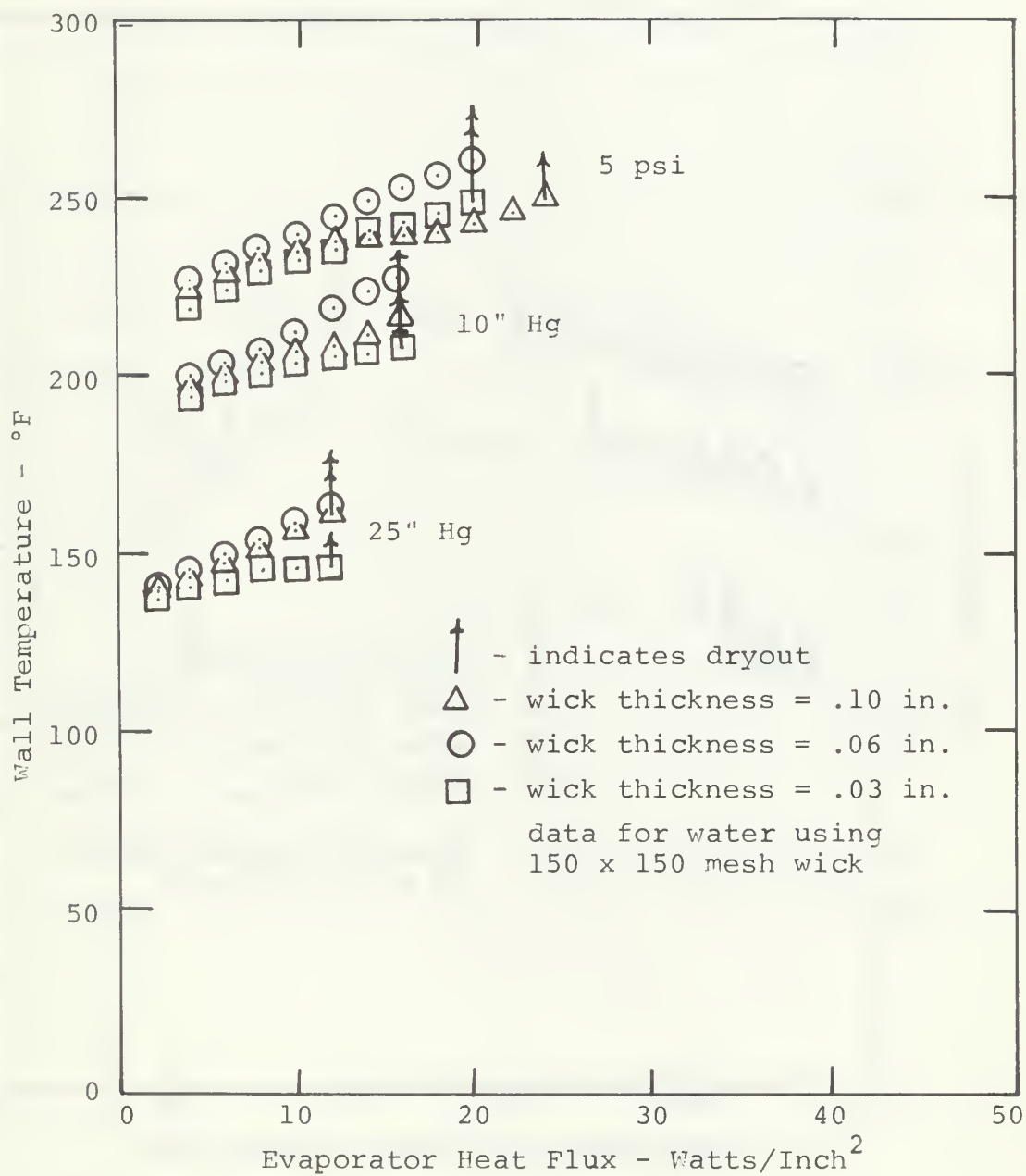
Figure 13. Heat Flux vs. Temperature
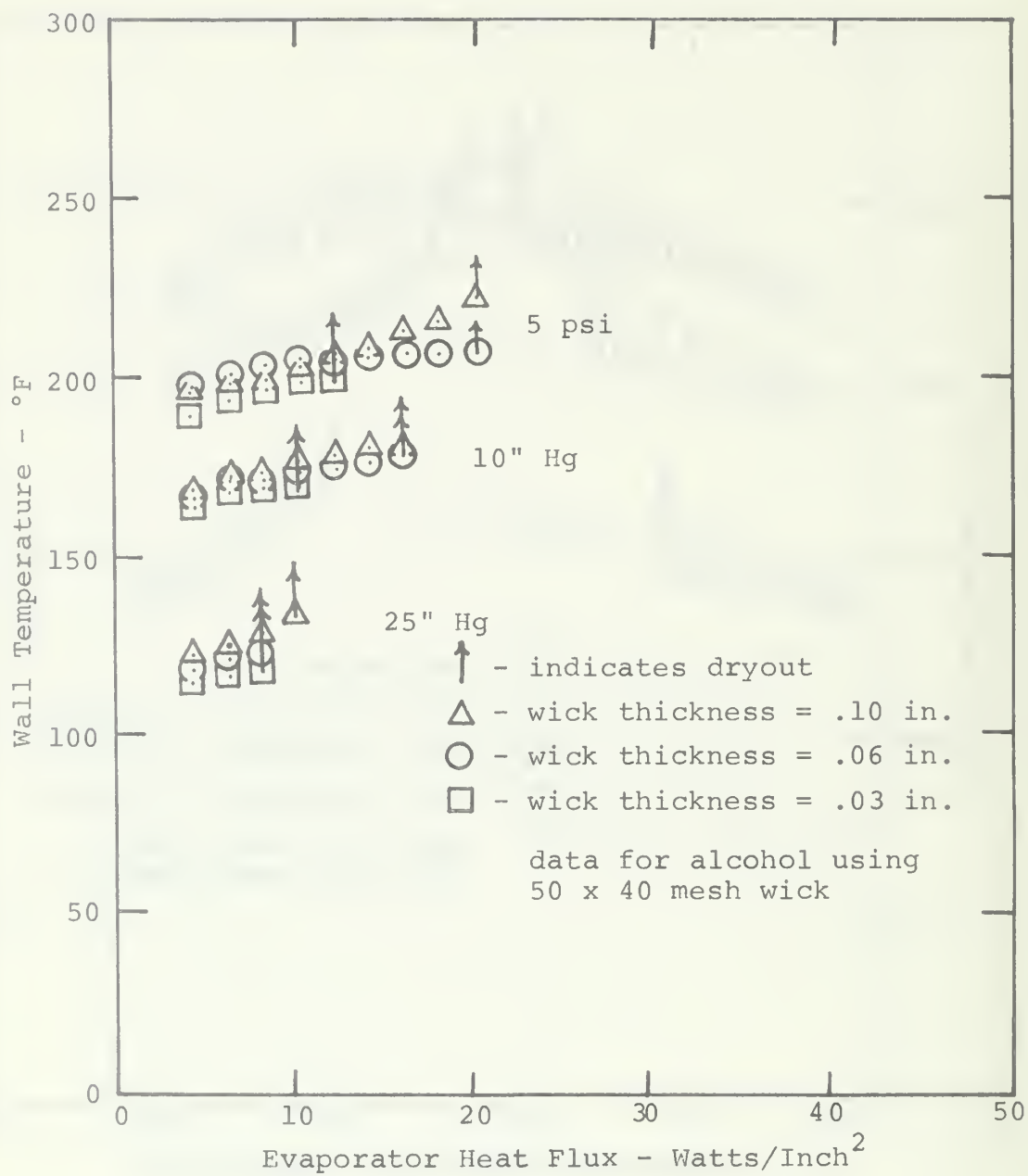
Figure 14. Heat Flux vs. Temperature
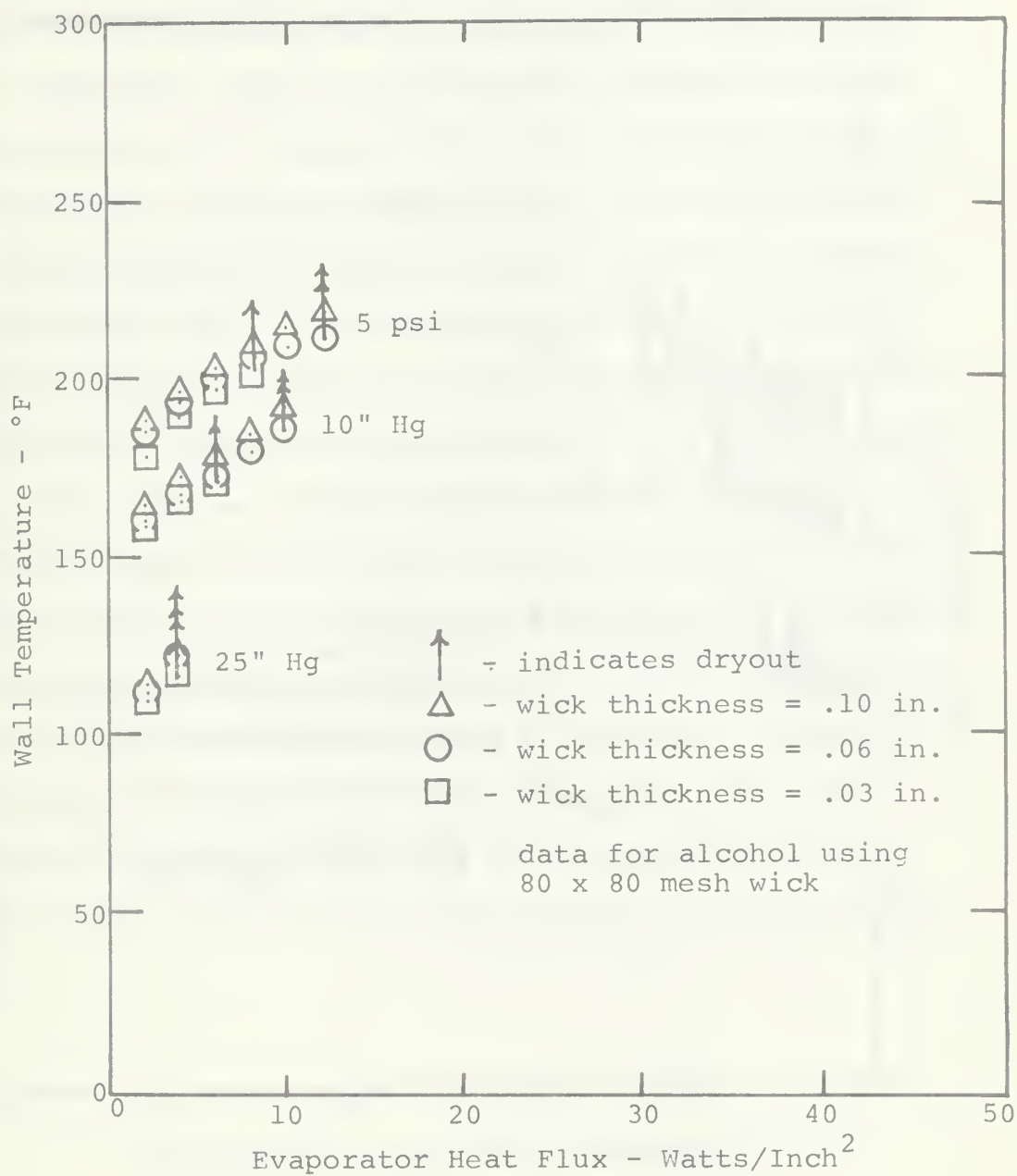
Figure 15. Heat Flux vs. Temperature
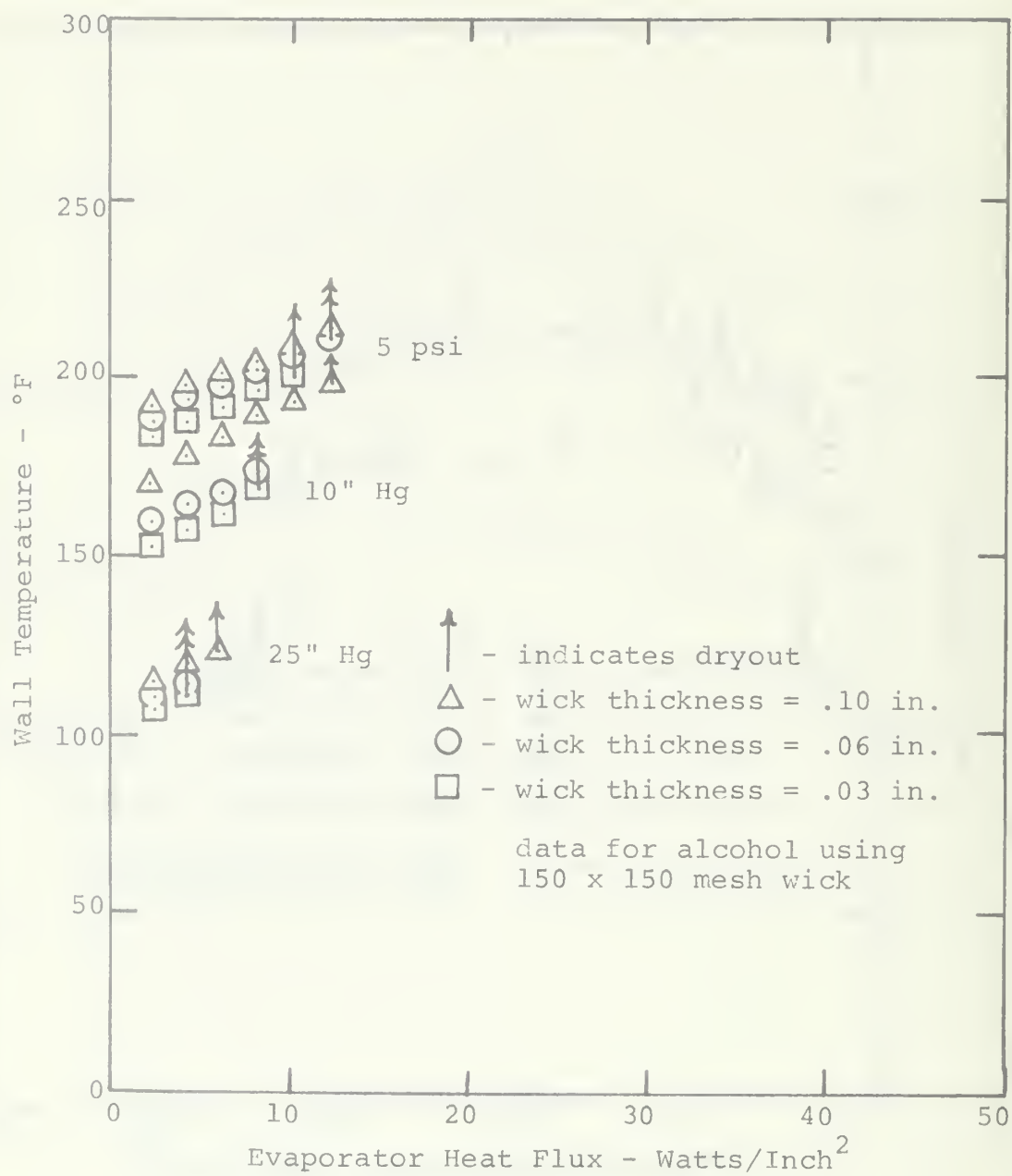
Figure 16. Heat Flux vs. Temperature

Figure 17. Heat Flux vs. Temperature

62

The three tests taken with the fifty mesh screen, at 25 inches Hg, were not consistent with theory or the other data obtained in this study. The pattern formed by these three tests indicates that Q_e increases with decreasing wick thickness. This is not the case, however, and the discrepancy can be linked to the aging problem. When data for the first tests was taken, with a wick thickness of .10 inches, premature dryout occurred since the wick was not properly aged. The discrepancy in the data was not noticed, however, until it was impossible to repeat the experiment. The same problem occurred with the one-fifty mesh wick, but was noticed immediately and corrected.

Since there were so many variables involved in equation (32), it was considered meaningless to attempt to evaluate theoretical values of Q_e. The most important point to be gotten from the data is the way in which Q_e varies when a certain parameter in equation (32) is changed. The trends predicted by the equation for the maximum heat transfer are quite evident in the experimental data.

VI. CONCLUSIONS

1. A wick, made of fifty mesh, plain weave, nickel wire cloth, can transfer more heat than a wick made of eighty or one-fifty mesh of the same material.

2. Increasing the wick thickness will increase the flow area in the wick. Dryout occurs at higher heat fluxes for a wick thickness of .10 inches than for wick thicknesses of .06 inches or .03 inches. The optimum value for the wick thickness in this pipe is predicted to be .186 inches.

3. Water is a better working fluid in heat pipes than ethyl alcohol, although alcohol has much better wetting characteristics.

4. The operating temperature of the heat pipe can be controlled by regulating the pressure. Dryout occurs at higher heat fluxes when the pressure is increased.

5. As the evaporator heat flux is increased the fluid level in the evaporator decreases.

6. The procedure for cleaning the screen was effective since there were no wetting problems observed between the wick and the working fluid.

VII.   RECOMMENDATIONS FOR FURTHER STUDY

1. Investigate the maximum heat transfer rates for wick thickness closer to the predicted optimum thickness of .186 inches.

2. Increase the inner radius of the glass envelope, obtain a new optimum thickness for the wick, and investigate the maximum heat transfer capabilities.

3. Obtain and test coarser meshes than the ones used in this study. This should decrease the magnitude of the pressure drop in the fluid, and result in higher dryout fluxes.

4. Put axial grooves in the pipe, and observe the maximum heat transfer rate as different size meshes are used to cover the grooves.

5. Investigate the effect that a shorter condenser would have on the system.

6. Insert a thermocouple into the wall of the pipe that would have the ability to traverse the length of the pipe.

7. Obtain a heater for use in the evaporator that has a much higher capacity than five-hundred watts.

Assume: (1) steady flow

(2) incompressible

(3) flow is symmetric

about the z-axis

(into the paper)

(4) $V_r = 0$

(5) $V_\theta = 0$
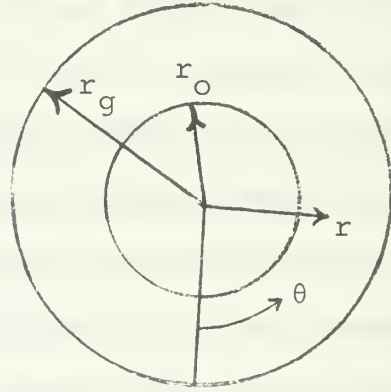
Boundary Conditions:

(1) at $r = r_g$, $V_z = 0$

(2) at $r = r_o$, $V_z = 0$

Continuity Equation:

$$\frac{1}{r} \frac{\partial}{\partial r} (rV_r) + \frac{1}{r} \frac{\partial V_\theta}{\partial \theta} + \frac{\partial V_z}{\partial z} = 0 \tag{1}$$

If $\qquad V_r = V_\theta = 0$, then $\dfrac{\partial V_z}{\partial z} = 0$

Momentum Equations:

$$r: \qquad 0 = \frac{1}{\rho} \frac{\partial p}{\partial r} \tag{2}$$

$$z: \qquad 0 = \frac{1}{\rho} \frac{\partial p}{\partial z} + \nu \frac{\partial^2 V_z}{\partial r^2} + \frac{\nu}{r} \frac{\partial V_z}{\partial r} \tag{3}$$

From equation (2) it is obvious that the pressure is only a function of z, and V_z is only a function or r. When equation (3) is rearranged, it gives

66

$$\frac{r}{\mu} \frac{dP}{dz} = \frac{\partial}{\partial r} \left(r \frac{\partial V_z}{\partial r} \right) \qquad (4)$$

Integrating both sides and rearranging gives

$$r \frac{\partial V_z}{\partial r} = \frac{r}{2\mu} \frac{dP}{dz} + \frac{A}{r} \qquad (5)$$

where A is a constant of integration.

Integrating again gives

$$V_z = \frac{r^2}{4\mu} \frac{dP}{dz} + A \ln r + B \qquad (6)$$

Boundary condition 1 yields

$$0 = B + A \ln r_g + \frac{r_g^2}{4\mu} \frac{dP}{dz} \qquad (7)$$

Boundary condition 2 yields

$$0 = B + A \ln r_o + \frac{r_o^2}{4\mu} \frac{dP}{dz} \qquad (8)$$

When equation (8) is subtracted from equation (7) the constant A can be solved for:

$$A = \frac{r_o^2 - r_g^2}{\ln r_g/r_o} \frac{1}{4\mu} \frac{dP}{dz} \qquad (9)$$

When equation (9) is substituted into equation (7) the constant B can be solved for:

$$B = \frac{r_g^2 - r_o^2}{\ln r_g/r_o} \frac{\ln(r_g)}{4\mu} \frac{dP}{dz} - \frac{r_g^2}{4\mu} \frac{dP}{dz} \qquad (10)$$

Substituting values for A and B into equation (6) yields

$$V_z = -\frac{dP}{dz}\frac{1}{4\mu}[r_g^2 - r^2 + \frac{r_g^2 - r_o^2}{\ln r_g/r_o}\ln\frac{r}{r_g}] \tag{11}$$

The mass flow rate is given by

$$\dot{m} = 2\pi\rho[\int_o^{r_g} r v_z dr - \int_o^{r_o} r v_z dr] \tag{12}$$

When equation (11) is substituted into equation (12) the mass flow rate becomes

$$\dot{m} = -\frac{dP}{dz}\frac{\pi\rho}{8\mu}[r_g^4 - r_o^4 - \frac{(r_g^2 - r_o^2)^2}{\ln r_o/r_g}] \tag{13}$$
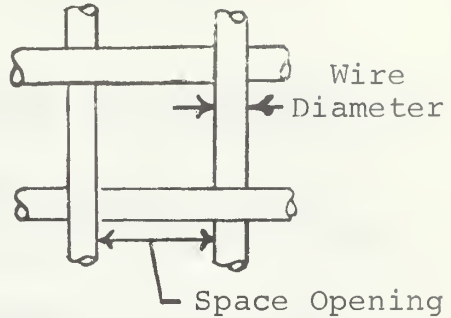
Therefore,

$$\frac{dP}{dz} = -\frac{\dot{m}8\mu}{\pi\rho}[\frac{1}{r_g^4 - r_o^4 - \frac{(r_g^2 - r_o^2)^2}{\ln r_o/r_g}}] \tag{14}$$

APPENDIX B: SAMPLE CALCULATIONS

Constants for the 80 mesh screen:

Wire Diameter = .007 inches

Space Opening = .0055 inches

Stacking Factor

Stacking factor is the average layer thickness divided by the wire diameter.

Four layers of stacked screen equals .055 inches.

$$\text{Stacking Factor} = \frac{.055/4}{.007} = 2.00$$

Porosity

Porosity is the percent of volume of the wick that is occupied by fluid.

The volume of one square inch of the wick is (1)(1) (.055) cubic inches. The volume of the wire is the mesh size times the number of layers times the volume of one wire.

$$\text{Wire Volume} = 2(4)(80)(\frac{.007}{2})^2 \; \pi = .0246 \text{ cubic inches}$$

$$\varepsilon = \frac{.055 - .0246}{.055} = 55.2\%$$

Surface Open Area

Surface open area is the percent of open area on one layer of screen.

$$\% \text{ Open Area} = (80)^2 (.0055)^2 = 19.4\%.$$

69

BIBLIOGRAPHY

1. Adamson, A. W., Physical Chemistry of Surfaces, Interscience, pp 4-6, 1960.

2. Air Force Flight Dynamics Laboratory Report AFFDL-TR-66-228, Cryogenic Heat Pipe, by W. L. Haskin, June 1967.

3. Burges, R. T., Design and Operation of a Heat Pipe, M.S. Thesis, Naval Postgraduate School, Monterey, California, 1968.

4. Carnesale, A., Cosgrove, J. H., and Ferrell, J. K., Operating Limits of the Heat Pipe, paper presented at AEC/Sandia Heat Pipe Conference, October 1966.

5. Eastman, G. Y., "The Heat Pipe," Scientific American, pp 38-46, May 1968.

6. Ernst, D. M., Evaluation of Theoretical Heat Pipe Performance, paper presented at the 1967 Thermionic Conversion Specialist Conference, Palo Alto, California, October 30-November 1, 1967.

7. Feldman, K. T. and Whiting, G. H., "The Heat Pipe," Mechanical Engineering, pp 30-33, February 1967.

8. Grover, G. M., Cotter, T. P., and Erickson, G. F., "Structures of Very High Thermal Conductance," Journal of Applied Physics, vol. 35, pp 1990-1991, 1964.

9. Katzoff, S., Notes on Heat Pipes and Vapor Chambers and Their Application to Thermal Control of Space-craft, paper presented at AEC/Sandia Heat Pipe Conference, October 1966.

10. Lawrence Radiation Laboratory, University of California, Livermore, UCRL - 50453, A Critical Review of Heat Pipe Theory and Applications, by H. Cheung, 15 July 1968.

11. Lawrence Radiation Laboratory, University of California, Livermore, UCRL - 50294, Heat Pipe Radiator for a 50-MWt Space Power Plant, by R. W. Werner and G. A Carlson, 30 June 1967.

12. Lewis Research Center, NASA CR - 812, Vapor - Chamber Fin Studies, Transport Properties and Boiling Characteristics of Wicks, by H. R. Kunz, L. S. Langston, B. H. Hilton, S. S. Wyde, and G. H. Nashick, June 1967.

13. Los Alamos Scientific Laboratory LA - 3585, Heat Pipe Capability Experiments, by J. E. Kemme, 1966.

14. Los Alamos Scientific Laboratory, University of California, Los Alamos, LA-3246-MS, Theory of Heat Pipes, by T. P. Cotter, February 1965.

15. Los Alamos Scientific Laboratory, University of California, Los Alamos, LA-3211, High Thermal Conductance Devices Utilizing the Boiling of Lithium or Silver, by J. E. Deverall and J. E. Kemme, 1965.

16. Mosteller, W. L., The Effect of Nucleate Boiling on Heat Pipe Operation, M. S. Thesis, Naval Postgraduate School, Monterey, California 1969.

17. Scheidegger, A. E., The Physics of Flow Through Porous Media, University of Toronto Press, 1960.

18. TRW Space Technology Laboratories Report No. 9895-6001-TU-000, On the Operation of Heat Pipes, by B. D. Marcus, May, 1965.

19. TRW Space Technology Laboratories Report No. N68-12857, An Analytical and Experimental Study of Heat Pipes, by L. G. Neal, January 1967.

20. Yuan, S. W. and Finklestein, A. B., "Laminar Flow with Injection and Suction Through a Porous Wall," Heat Transfer and Fluid Mechanics Institute, Los Angeles, California 1955.

INITIAL DISTRIBUTION LIST

		No. Copies
1.	Defense Documentation Center Cameron Station Alexandria, Virginia 22314	20
2.	Library Naval Postgraduate School Monterey, California 93940	2
3.	Naval Ships System Command (Code 2052) Navy Department Washington, D. C. 20360	1
4.	Mechanical Engineering Department Naval Postgraduate School Monterey, California 93940	2
5.	Professor P. F. Pucci Mechanical Engineering Department Naval Postgraduate School Monterey, California 93940	1
6.	Professor P. J. Marto Mechanical Engineering Department Naval Postgraduate School Monterey, California 93940	1
7.	LTJG Hugh E. Kilmartin, Jr., U.S.N. Naval Nuclear Power School Naval Training Command Bainbridge, Maryland 21905	2
8.	LT. W. L. Mosteller, U.S.N. Fleet Activities, Sasebo c/o Fleet Post Office Seattle, Washington 98766	1

DOCUMENT CONTROL DATA - R & D

(Security classification of title, body of abstract and indexing annotation must be entered when the overall report is classified)

1. ORIGINATING ACTIVITY *(Corporate author)*	2a. REPORT SECURITY CLASSIFICATION
Naval Postgraduate School Monterey, California 93940	Unclassified
	2b. GROUP

3. REPORT TITLE

THE EFFECT OF WICK GEOMETRY ON THE
OPERATION OF A LONGITUDINAL HEAT PIPE

4. DESCRIPTIVE NOTES *(Type of report and inclusive dates)*
Masters Thesis, June 1969

5. AUTHOR(S) *(First name, middle initial, last name)*

Hugh Edward Kilmartin, Jr., Lieutenant (junior grade), USN

6. REPORT DATE	7a. TOTAL NO. OF PAGES	7b. NO. OF REFS
June 1969	70	20

8a. CONTRACT OR GRANT NO.	9a. ORIGINATOR'S REPORT NUMBER(S)
b. PROJECT NO.	
c.	9b. OTHER REPORT NO(S) *(Any other numbers that may be assigned this report)*
d.	

10. DISTRIBUTION STATEMENT

Distribution of this document is unlimited.

11. SUPPLEMENTARY NOTES	12. SPONSORING MILITARY ACTIVITY
	Naval Postgraduate School Monterey, California 93940

13. ABSTRACT

   Evaporative heat transfer limits were obtained and
studied for an everted heat pipe with varying wick geo-
metries. The wick geometries were a function of the wire
mesh size and the total wick thickness.

   A nickel heat pipe was built and operated using both
water and ethyl alcohol as the working fluids. The
different wick materials used were 50 mesh, 80 mesh, and
150 mesh, plain weave, nickel wire cloth. The scope of
the investigation included operating the pipe at 25 inches
mercury vacuum, 10 inches mercury vacuum, and 5 pounds
per square inch gage.

   The maximum heat transfer was found to increase as
the mesh size was decreased, as the wick thickness was
increased, or as the pressure was increased.

   The equipment used to obtain experimental data is
described and experimental results and sample calculations
are presented.

DD FORM 1 NOV 65 **1473** (PAGE 1)

S/N 0101-807-6811

A-31408

KEY WORDS	LINK A		LINK B		LINK C	
	ROLE	WT	ROLE	WT	ROLE	WT
HEAT PIPE						
WICKING MATERIALS						